

# Fundamentals of Advanced Planarization: Pad Micro-Texture, Pad Conditioning, Slurry Flow, and Retaining Ring Geometry

*(Task 425.032)*

## Subtask 1: Effect of Retaining Ring Geometry on Slurry Flow and Pad Micro-Texture

### PI:

- Ara Philipossian, Chemical and Environment Engineering, UA

### Graduate Student:

- Xiaoyan Liao, Ph. D. candidate, Chemical and Environmental Engineering, UA

### Other Researchers:

- Yasa Sampurno, Postdoctoral Fellow, Chemical and Environment Engineering, UA
- Yun Zhuang, Postdoctoral Fellow, Chemical and Environment Engineering, UA

# Fundamentals of Advanced Planarization: Pad Micro-Texture, Pad Conditioning, Slurry Flow, and Retaining Ring Geometry

*(Task 425.032)*

## Subtask 1: Effect of Retaining Ring Geometry on Slurry Flow and Pad Micro-Texture

### Cost Share (other than core ERC funding):

- **In-kind donation (retaining rings) from Entegris, Inc.**
- **In-kind donation (slurry) from Fujimi Corporation**
- **In-kind support (bow wave image analysis) from Araca, Inc.**

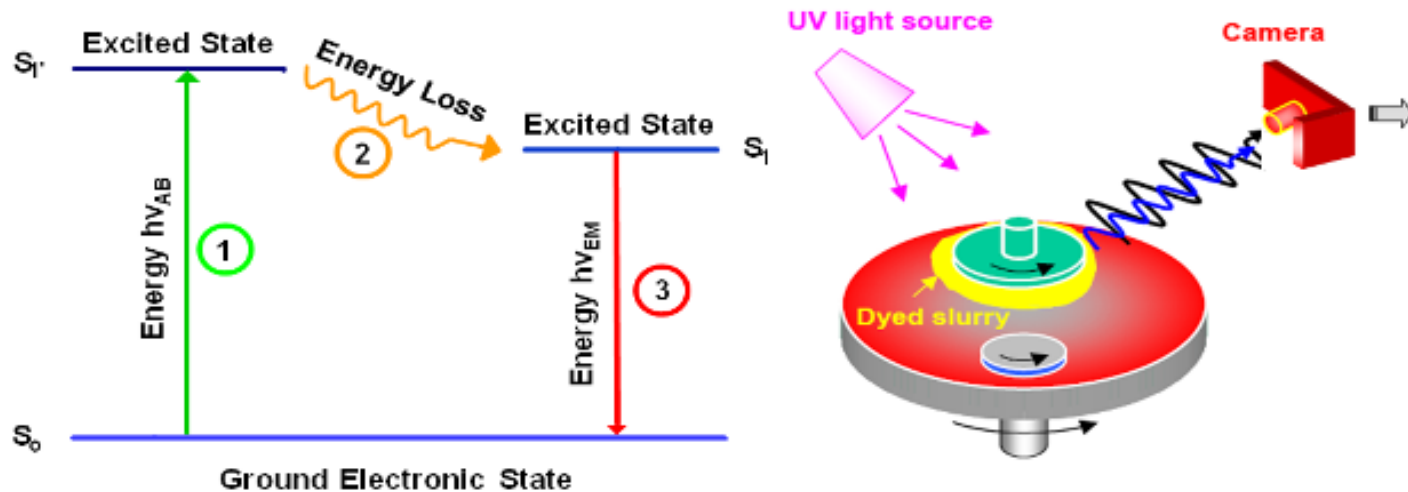
# Objectives and EHS Impact

- **Develop UV enhanced fluorescence system and quantify the extent of fluorescent light emitted by the slurry**
- **Employ the fluorescent light data to rapidly assess slurry flow patterns as a function of slurry application/injection schemes, retaining ring designs, slurry flow rates, pad groove designs and tool kinematics**
- **Investigate the effect of slurry application/injection schemes, retaining ring slot design and polishing conditions including pad/retaining ring sliding velocity, retaining ring pressure and slurry flow rate on fluid dynamics at the bow wave**

**EHS Impact – Reduce slurry consumption by 40 percent through more efficient slurry delivery to the pad-wafer interface**

# General Approach

- Tag slurry with a special set of fluorescent dyes
- Use UV – LED as light sources to excite the dyes in the slurry causing them to emit fluorescent light
- Employ a high resolution CCD camera to record the emission of fluorescent light
- Develop software and quantitatively assess the flow pattern using the movie from CCD camera



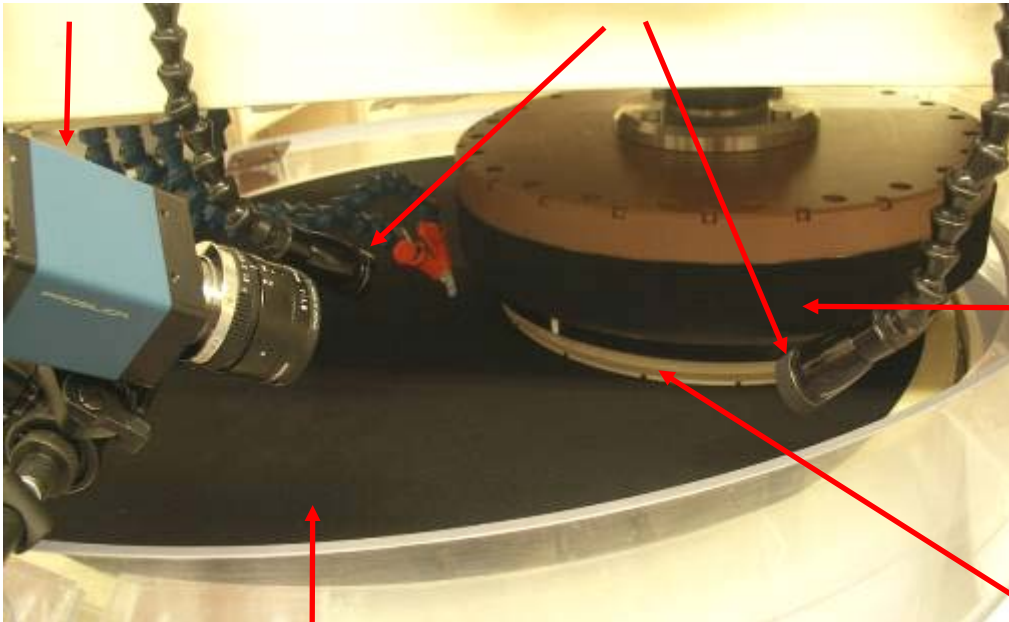
Jablonski Energy Level Diagram

UV Fluorescence Technique

# Experimental Setup

**HD CCD Camera**

**UV Lights**



**Polisher** : Araca APD – 800®  
**Camera shutter** : 0.02 sec  
**Frequency** : 5 Hz  
**Frames per run** : 50 frames

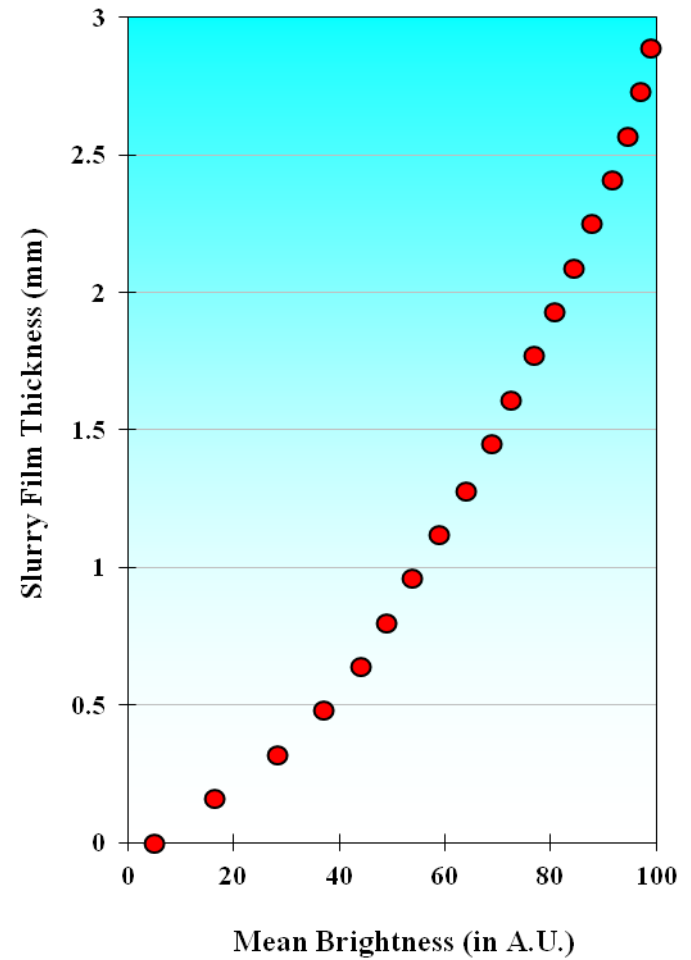
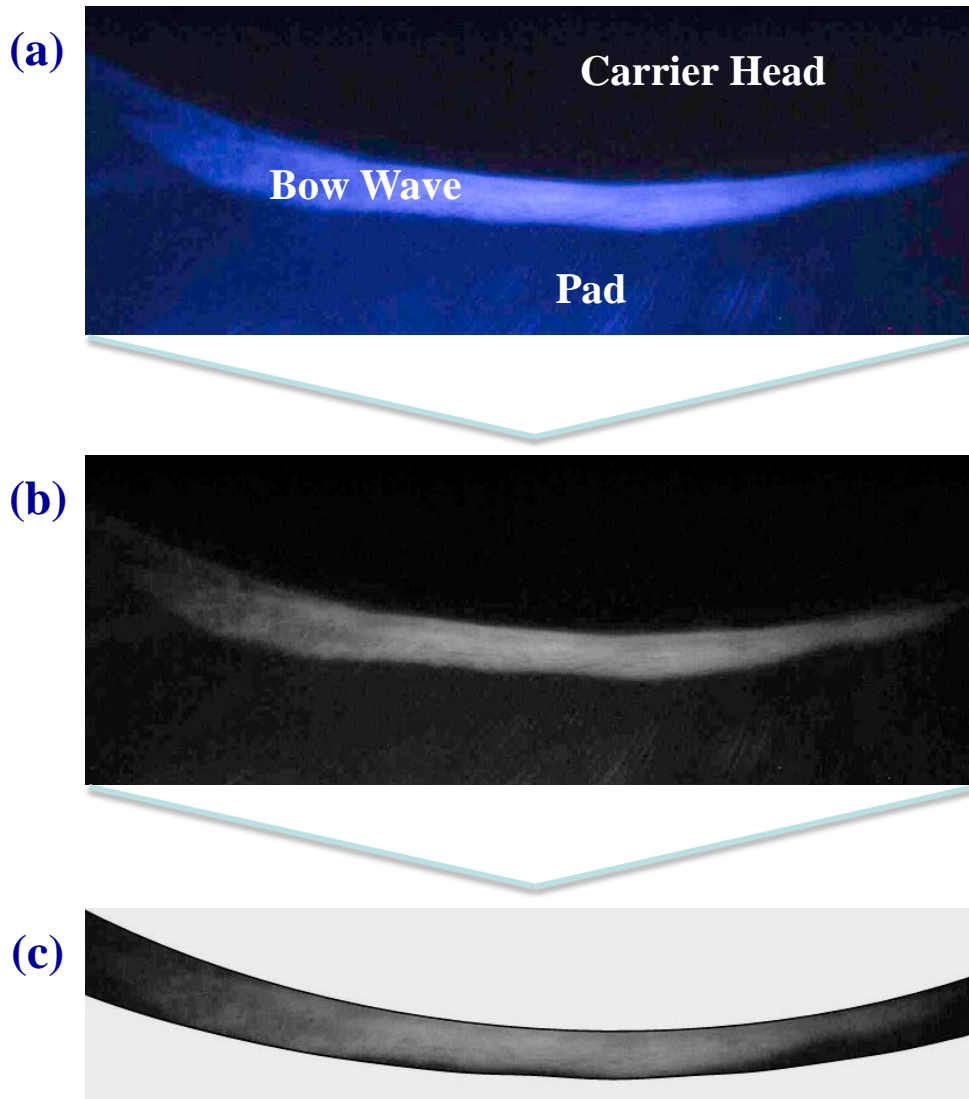
**Carrier Head**



**Politex Pad**

**Retaining Ring**

# Bow Wave Thickness Measurement – UVIZ



# Experimental Conditions

- **Slurry Application/Injection Methods**
  - **Standard pad center area application method**
  - **Novel slurry injection system**
- **Retaining Ring Designs**
  - **PEEK-1 and PEEK-2**
- **Sliding Velocities**
  - **0.6 and 1.2 m/s**
- **Ring Pressures**
  - **1.9 and 3.8 PSI**
- **Slurry Flow Rates**
  - **150 and 300 ml/min**
- **Pad**
  - **Dow Electronic Materials Politex REG**
- **Pad Conditioning**
  - **In-situ conditioning at 3 lb<sub>f</sub> by 3M PB32A brush**
- **Slurry**
  - **1 part of Fujimi PL-7103 slurry + 4 parts of DI H<sub>2</sub>O + 0.5 g/L Coumarin (4-Methylumbelliferone)**
- **Polishing Time**
  - **20 seconds**

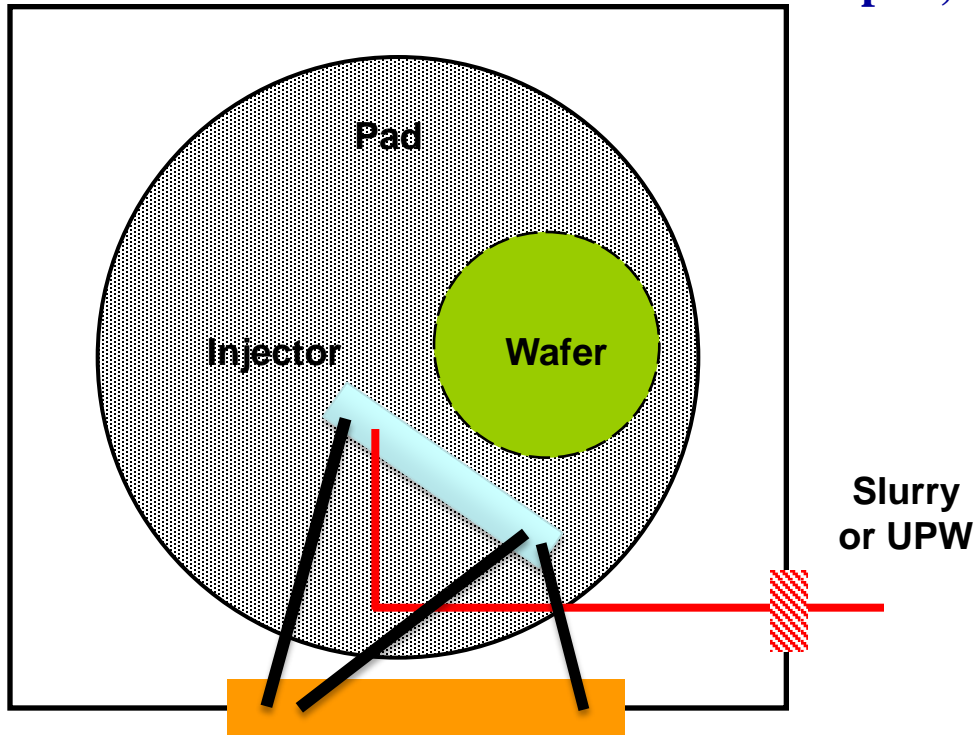
# Novel Slurry Injector System (SIS)

Slurry injector system is placed on top of the pad; fresh slurry is applied over the wafer track in a thin film through the SIS.

**More efficient slurry delivery**

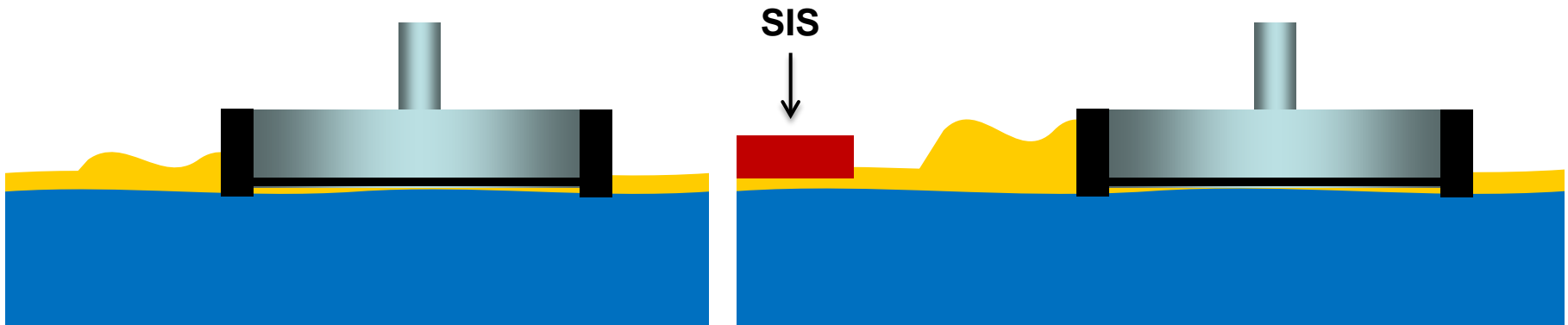
**Higher material removal rate**

**Lower polishing defects**



# Bow Wave in CMP

- Higher bow wave at the retaining ring suggests greater slurry availability.
- Greater slurry availability suggests more effective delivery of slurry to the wafer-pad interface where polishing is taking place.



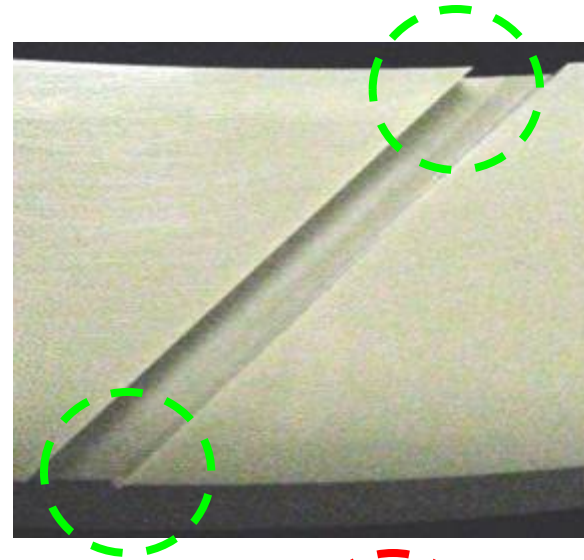
**With Point Application**

**With SIS**

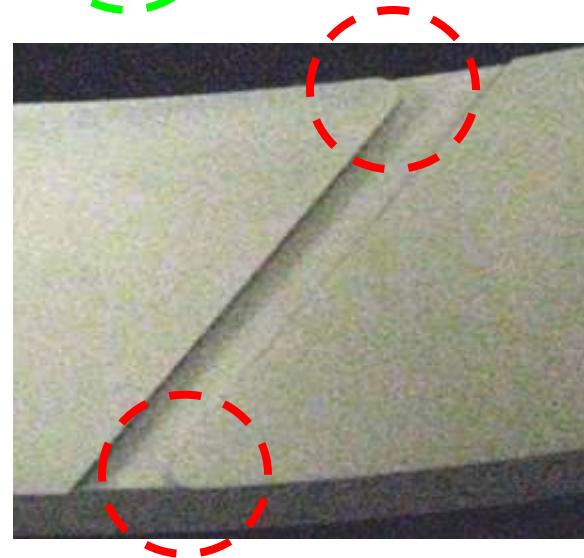
# Retaining Ring Slot Designs



**Retaining Ring for 300-mm Wafer Process**



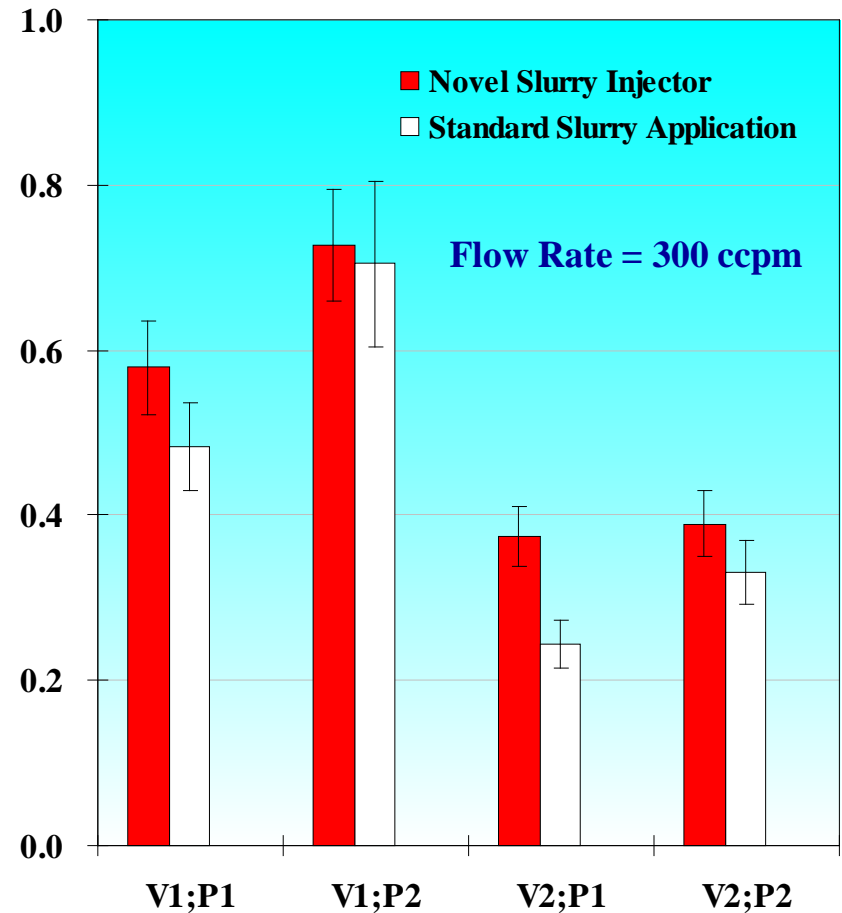
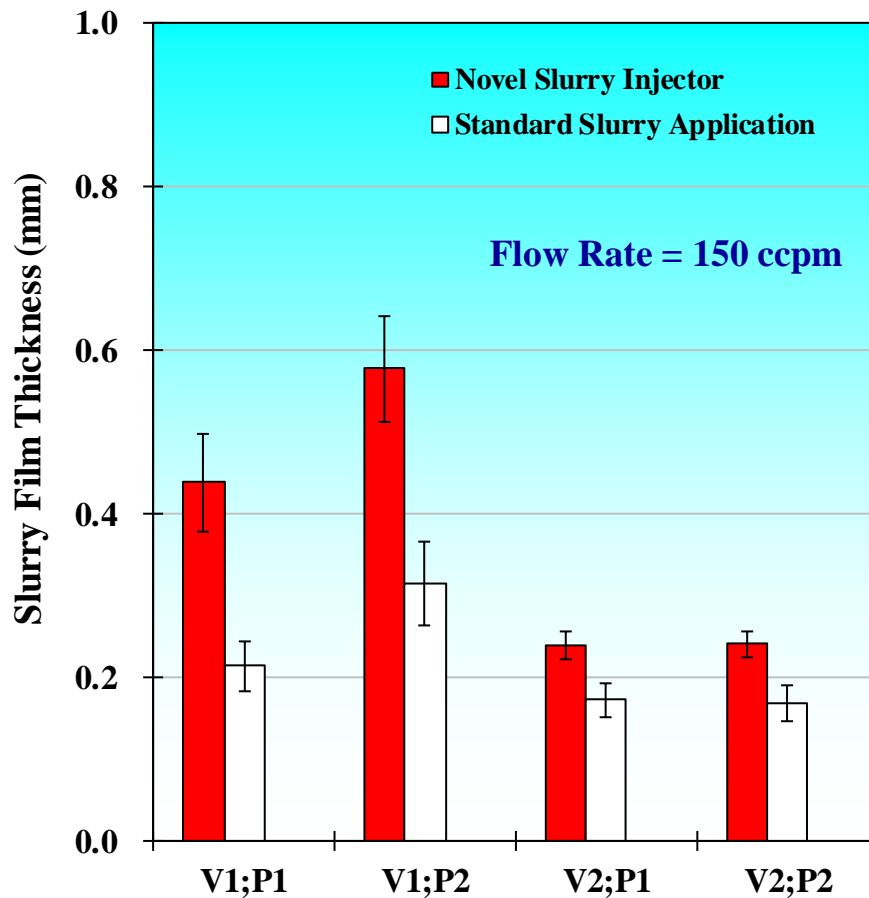
**PEEK-1**



**PEEK-2**

# Bow Wave Slurry Film Thickness

## Effect of Slurry Application/Injection Scheme for PEEK-1



**V1 = 0.6 m/s ; V2 = 1.2 m/s ; P1 = 1.9 PSI ; P2 = 3.8 PSI**

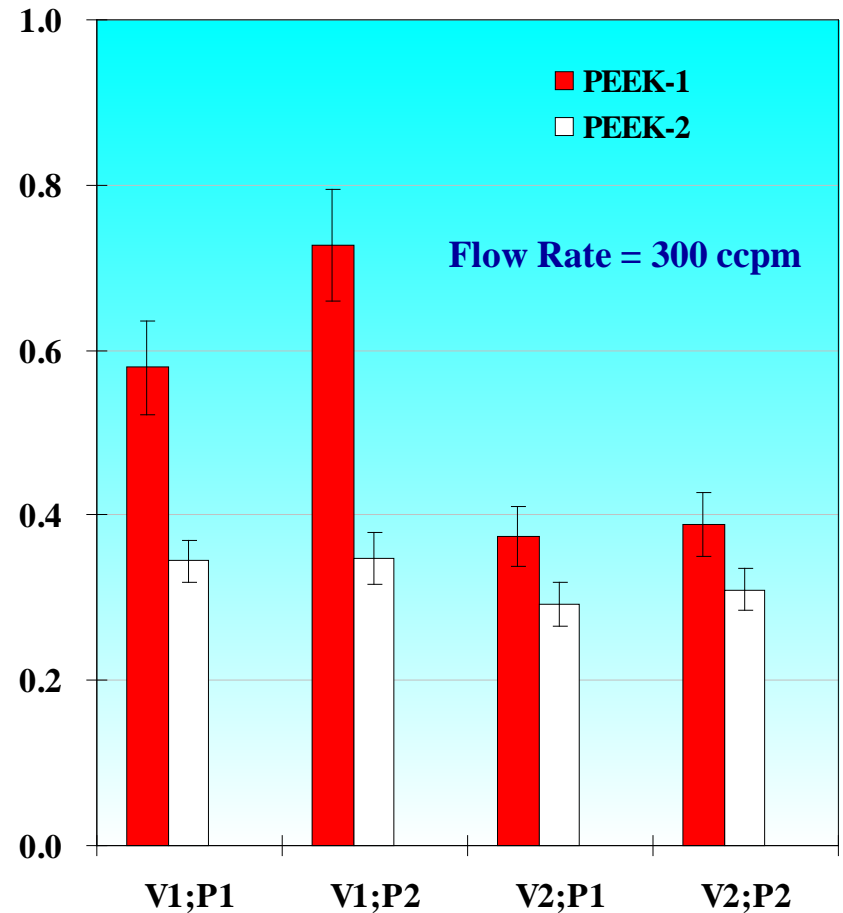
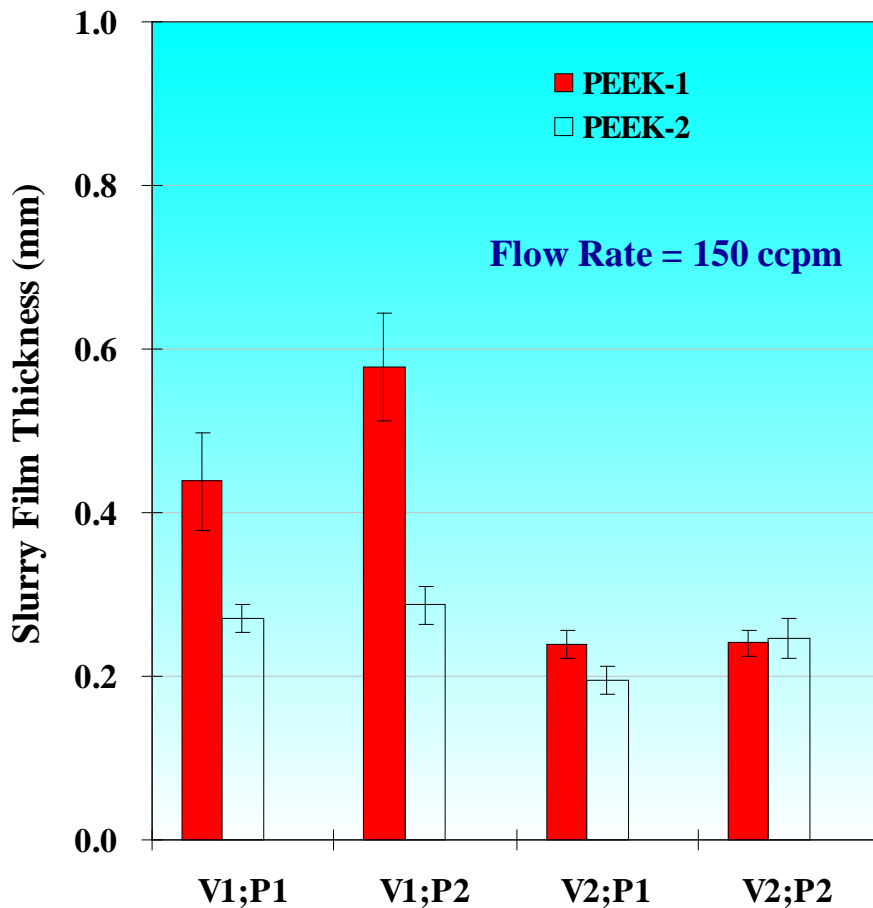
**Note: Politex pad with the retaining ring contacting the pad.**

## Rough Estimate of Slurry Savings

- **Assuming that there is bow wave thickness equivalence between the SIS and Point Application, UVIZ results indicate that:**
  - ✓ **At 0.6 m/s and 1.9 PSI, same slurry bow wave thickness can be achieved with only 198 ml/min using SIS, compared to 300 ml/min using Point Application (34 percent savings).**
  - ✓ **When pressure is doubled, slurry savings with SIS are 8 percent.**
  - ✓ **At 1.2 m/s and 1.9 PSI, same slurry bow wave thickness can be achieved with 157 ml/min using SIS, compared to 300 ml/min with Point Application (48 percent savings).**
  - ✓ **At 3.8 PSI, slurry savings with SIS is approximately 20 percent.**

# Bow Wave Slurry Film Thickness

## Effect of Retaining Ring Design for SIS



**V1 = 0.6 m/s ; V2 = 1.2 m/s ; P1 = 1.9 PSI ; P2 = 3.8 PSI**  
**Note: Politex pad with the retaining ring is contacting the pad.**

# Slurry Film Comparison for Retaining Ring Design

- **Comparing the bow wave thickness between PEEK-1 and PEEK-2 retaining rings, UVIZ results indicate that:**
  - ✓ **Retaining ring with the sharp angle slot design (PEEK-1) generated thicker slurry films at the bow wave in 7 out of 8 cases than PEEK-2 which had a rounded angle slot design.**
  - ✓ **For PEEK-1, slurry film thickness at the bow wave increased with increasing flow rate and ring pressure while it decreased with increasing pad/retaining ring sliding velocity.**
  - ✓ **For PEEK-2, slurry film thickness at the bow wave did not change significantly under different polishing conditions indicating an apparent robustness of the PEEK-2 design to various operating conditions.**

## Summary

- **Slurry film thickness at the bow wave was successfully measured by the UVIZ - 100 system using UV fluorescence methods.**
- **For both PEEK-1 and PEEK-2 retaining rings, the slurry injection system generated consistently thicker bow waves and provided greater slurry availability at different polishing conditions compared to the standard pad center area application method.**
- **For the slurry injection system, PEEK-2 retaining ring generated consistently thinner bow wave than PEEK-1, suggesting that its rounded angle slots facilitated slurry transport in the pad-wafer interface. In addition, slurry film thickness at the bow wave did not change significantly at different polishing conditions indicating an apparent robustness of the PEEK-2 design to various operating conditions.**
- **We achieved our goal of reducing slurry consumption by 40% through more efficient slurry delivery to the pad-wafer interface.**

# Industrial Interactions

## Industrial mentors and contacts:

- Christopher Wargo (Entegris)
- Joseph Smith (Entegris)

## Publications and Presentations

- **Effects of Slurry Application/Injection Schemes on Slurry Availability during Chemical Mechanical Planarization (CMP), X. Liao, Y. Sampurno, Y. Zhuang and A. Philipossian. Electrochemical and Solid-State Letters, 15(4), H118-122, 2012.**
- **Effect of Slurry Application/Injection Methods and Polishing Conditions on Bow Wave Characteristics, X. Liao, Y. Sampurno, Y. Zhuang, F. Sudargho, A. Rice and A. Philipossian. ECS Transactions, 34(1), 659-663, 2011.**
- **Effect of Slurry Application/Injection Methods, Retaining Ring Slot Designs, and Polishing Conditions on Bow Wave Fluid Dynamics, X. Liao, Y. Sampurno, Y. Zhuang, F. Sudargho, A. Rice and A. Philipossian. China Semiconductor Technology International Conference, Shanghai, China, March 13-14, 2011.**

# Fundamentals of Advanced Planarization: Pad Micro-Texture, Pad Conditioning, Slurry Flow, and Retaining Ring Geometry

*(Task 425.032)*

## Subtask 2: Effect of Pad Conditioning on Pad Micro-Texture and Polishing Performance

### PI:

- Ara Philipossian, Chemical and Environment Engineering, UA

### Graduate Students:

- Xiaoyan Liao, Ph. D. candidate, Chemical and Environment Engineering, UA
- Yubo Jiao, Ph. D. candidate, Chemical and Environment Engineering, UA
- Changhong Wu, Ph. D. candidate, Chemical and Environment Engineering, UA
- Anand Meled, graduated with Ph. D. from UA in May 2011

# Fundamentals of Advanced Planarization: Pad Micro-Texture, Pad Conditioning, Slurry Flow, and Retaining Ring Geometry

*(Task 425.032)*

## Subtask 2: Effect of Pad Conditioning on Pad Micro-Texture and Polishing Performance

### Other Researchers:

- **Yun Zhuang, Post-doctoral Fellow, Chemical and Environment Engineering, UA**
- **Yasa Sampurno, Post-doctoral Fellow, Chemical and Environment Engineering, UA**

### Cost Share (other than core ERC funding):

- **In-kind donation (slurry) from Cabot Microelectronics Corporation**
- **In-kind donation (slurry) from DA NanoMaterials**
- **In-kind support (confocal microscopy) from Araca, Inc.**

# Objectives and EHS Impact

- **Investigate the effect of pad conditioning on pad surface micro-texture, as well as frictional force and removal rate during copper CMP process**

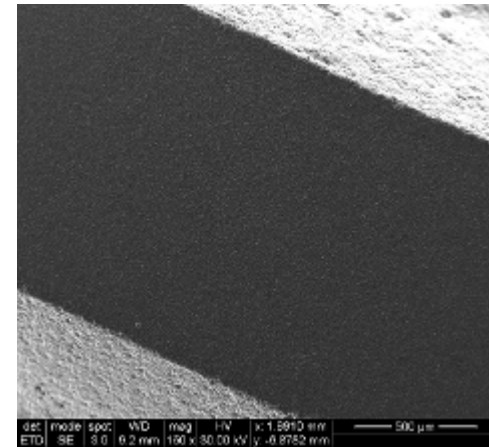
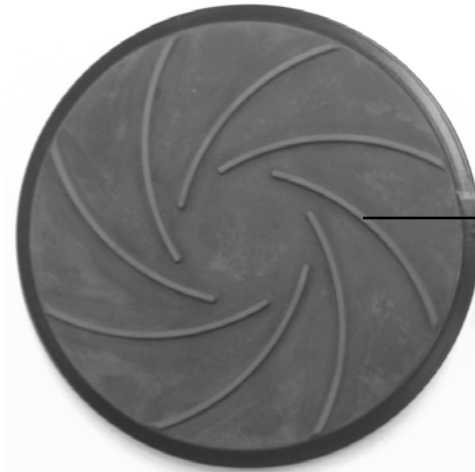
**EHS Impact – Reduce CMP consumable consumption (pad, slurry, UPW, chemicals, pad conditioner, and retaining ring) by 10 percent (due to RR increase caused by better pad conditioning)**

## General Approach

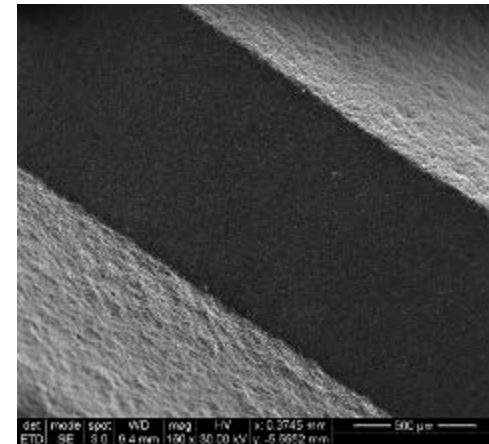
**Polish 300-mm blanket copper wafers with two different Morgan Technical Ceramics CVD discs, and analyze pad micro-texture through laser confocal microscopy.**

# Morgan Technical Ceramics CVD Discs

**Disc 4S850LF5**

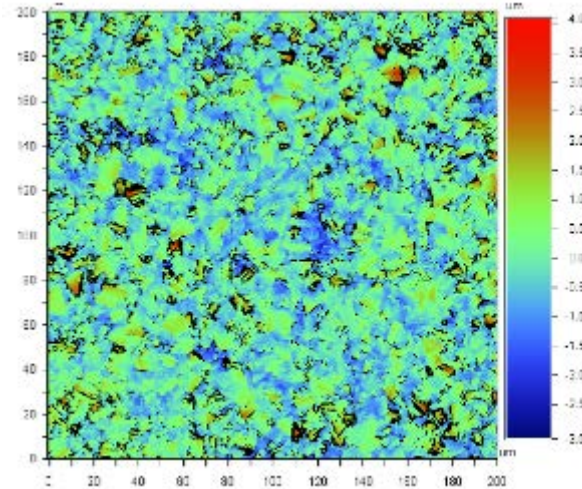
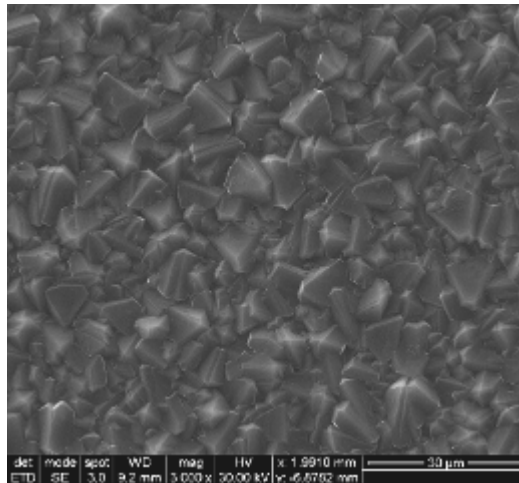


**Disc 4S835LF5**



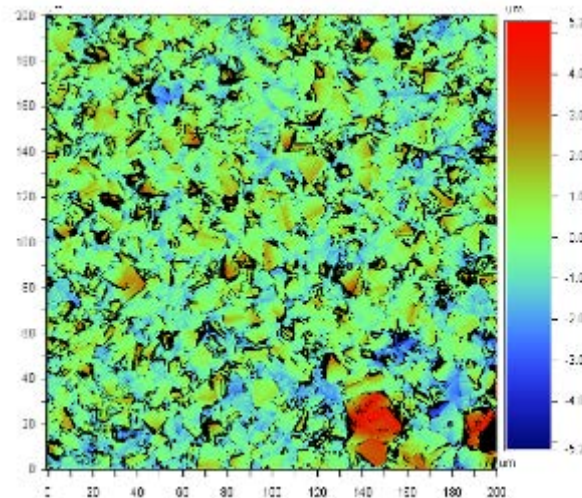
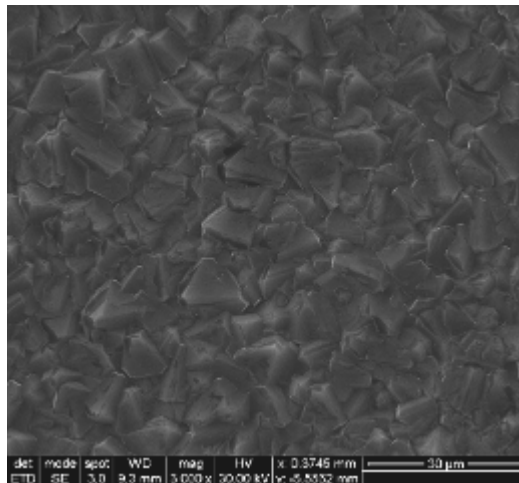
# Morgan Technical Ceramics CVD Discs

Disc 4S850LF5



Average Surface Roughness  
553 nm

Disc 4S835LF5



Average Surface Roughness  
758 nm

# Polishing Conditions

## – Pad

- Cabot Microelectronics Corporation D100 31” concentrically grooved pad

## – Wafer

- 300-mm blanket Cu wafer

## – Slurry

- 345.6 volume parts of DANano CU 3900 slurry + 622.1 volume parts of DI H<sub>2</sub>O + 32.3 volume parts of 30% ultra pure H<sub>2</sub>O<sub>2</sub>
- Flow rate: 300 ml/min

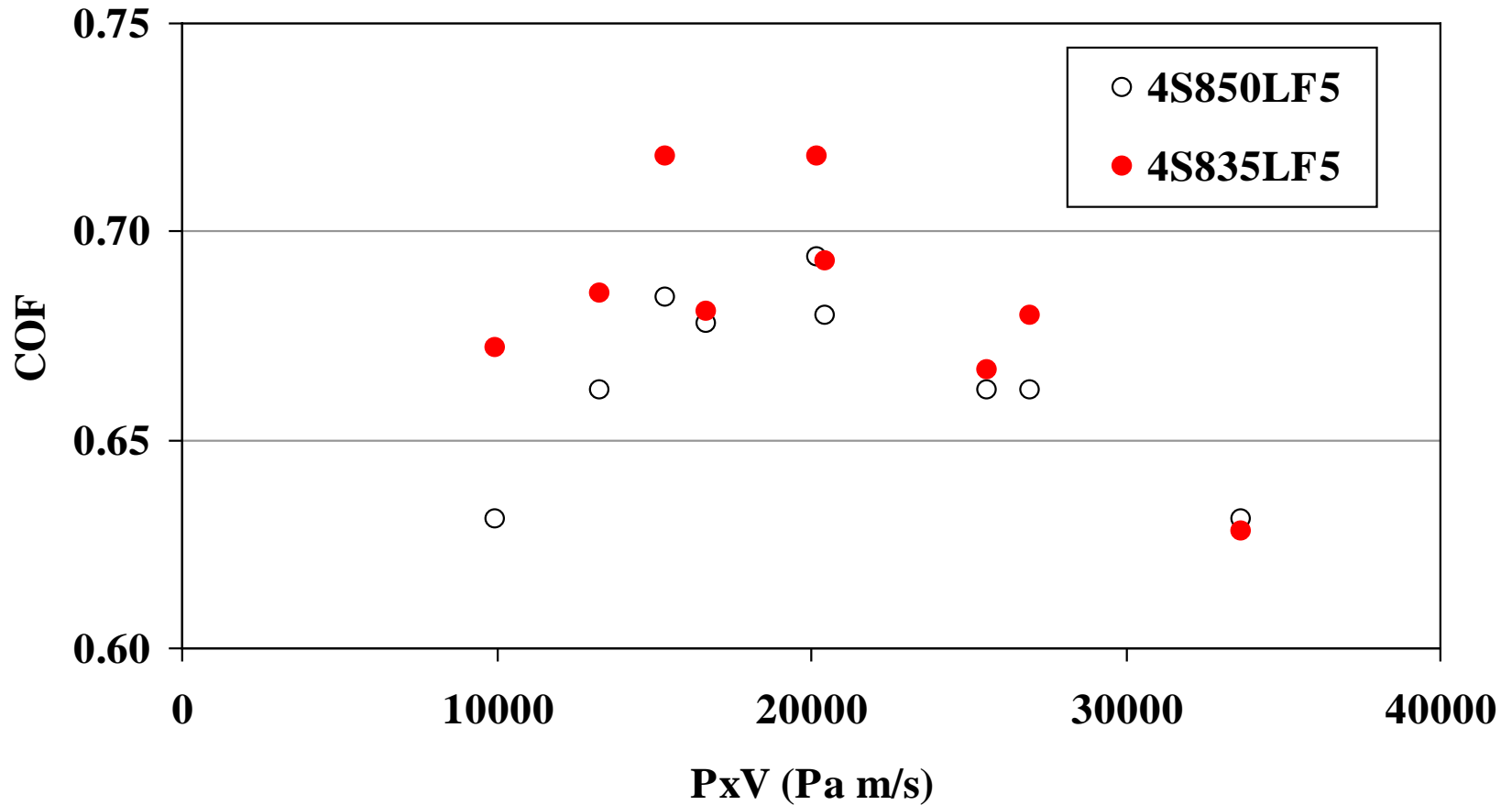
## – Pad Conditioning

- Disc 4S850LF5 and Disc 4S835LF5 rotating at 95 RPM and sweeping at 10 times/min
- In-situ pad conditioning at 6 lb<sub>f</sub>

## – Polishing Conditions

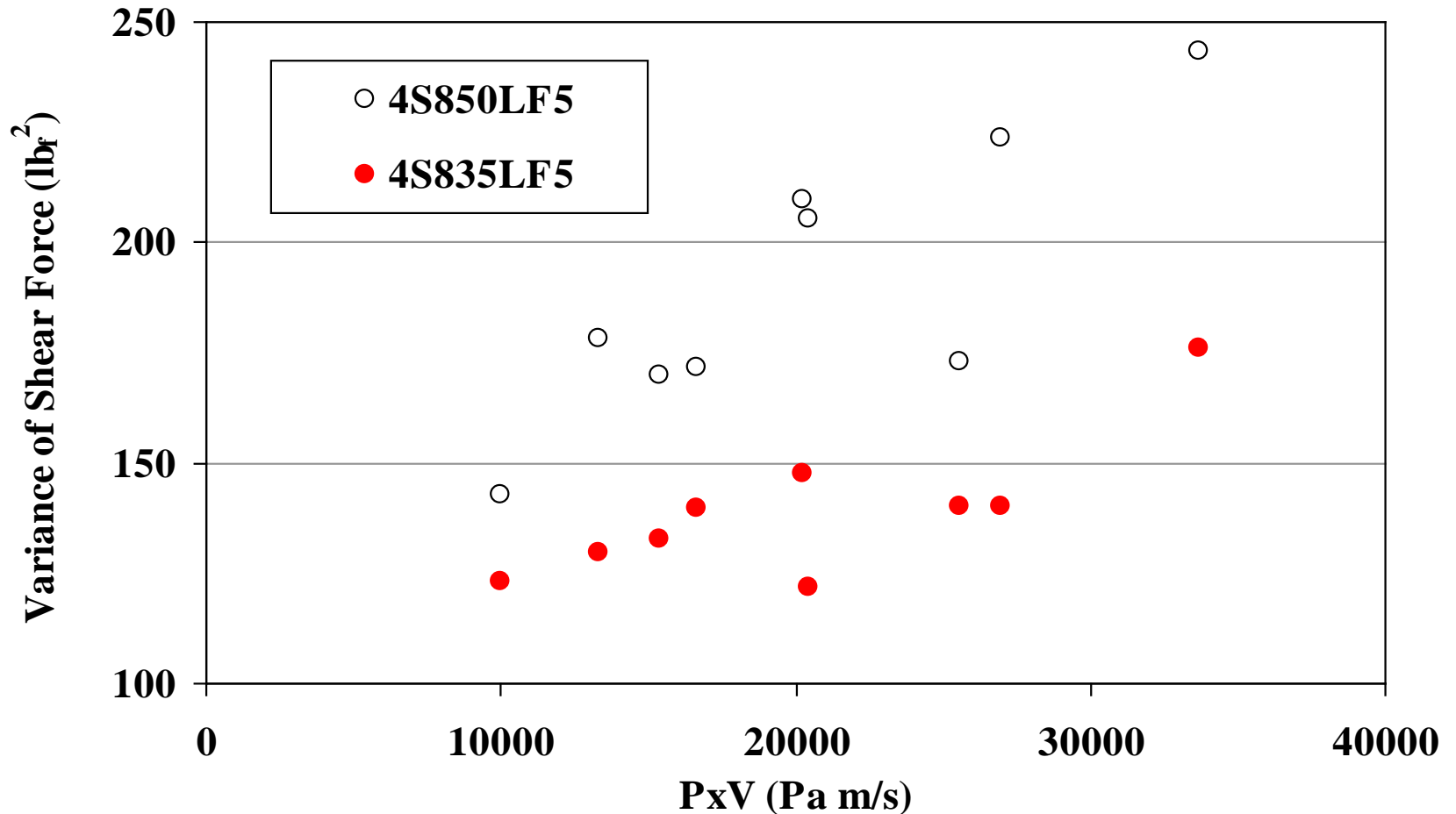
- Polishing pressure: 1.5, 2.0 and 2.5 PSI
- Sliding velocity: 1, 1.5, and 2 m/s
- Polishing time: 1 minute

# Coefficient of Friction



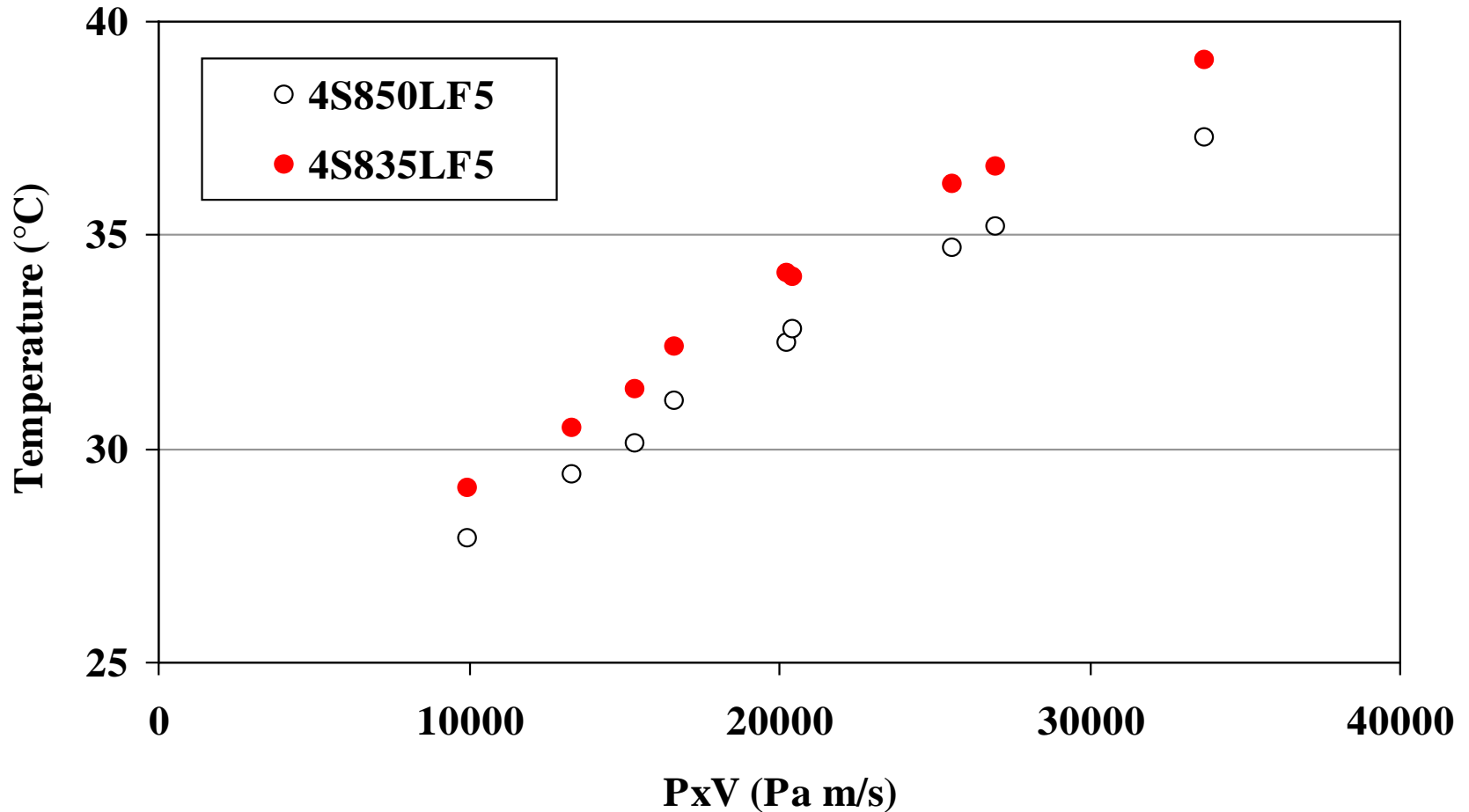
**In general, Disc 4S835LF5 generated higher COFs than Disc 4S850LF5.**

# Variance of Shear Force



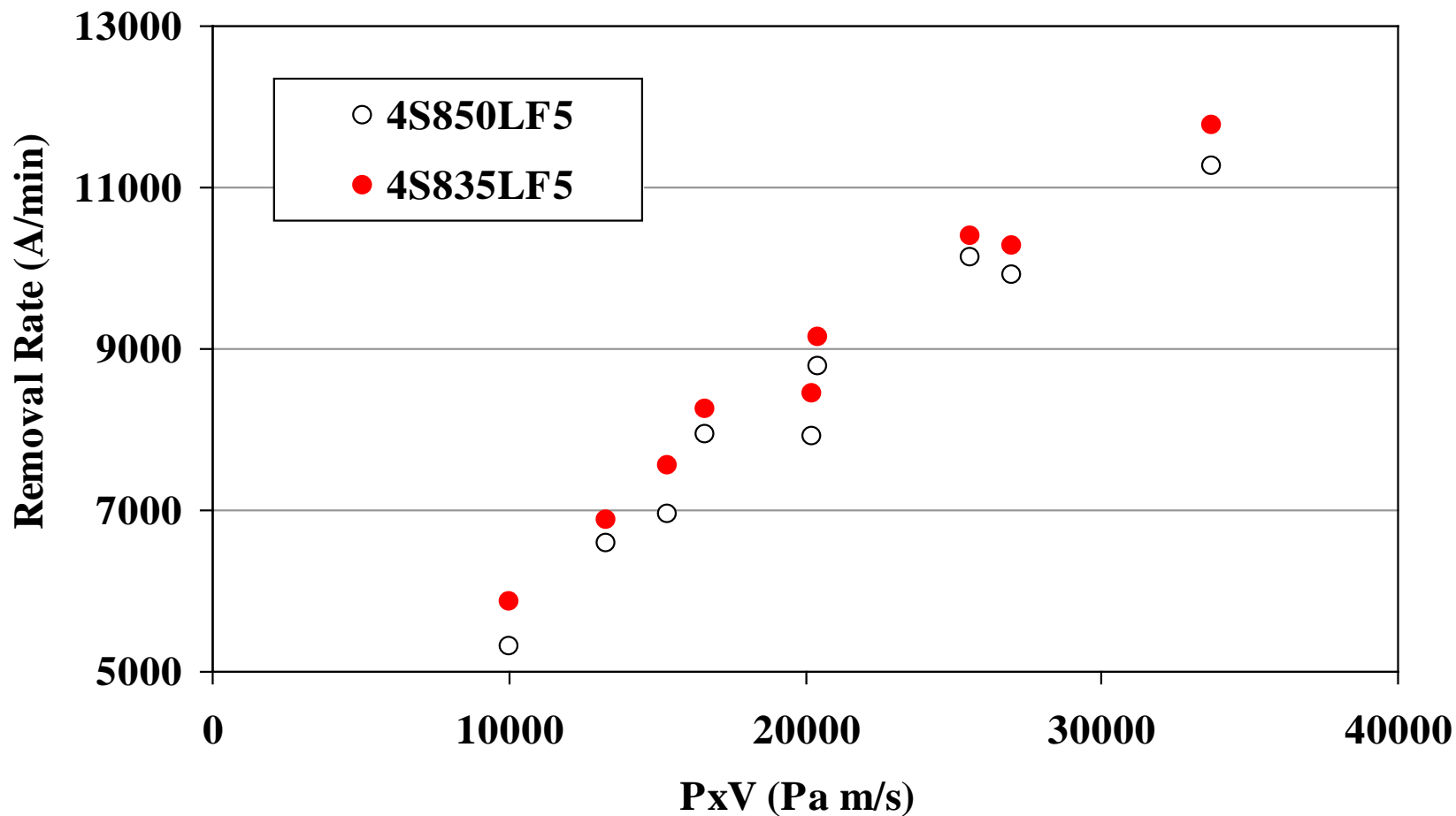
**Disc 4S835LF5 generated lower variance of shear forces than Disc 4S850LF5.**

# Mean Pad Temperature



**Disc 4S835LF5 generated higher pad temperatures than Disc 4S850LF5.**

# Copper Removal Rate



**Disc 4S835LF5 generated higher removal rates Disc 4S850LF5.**

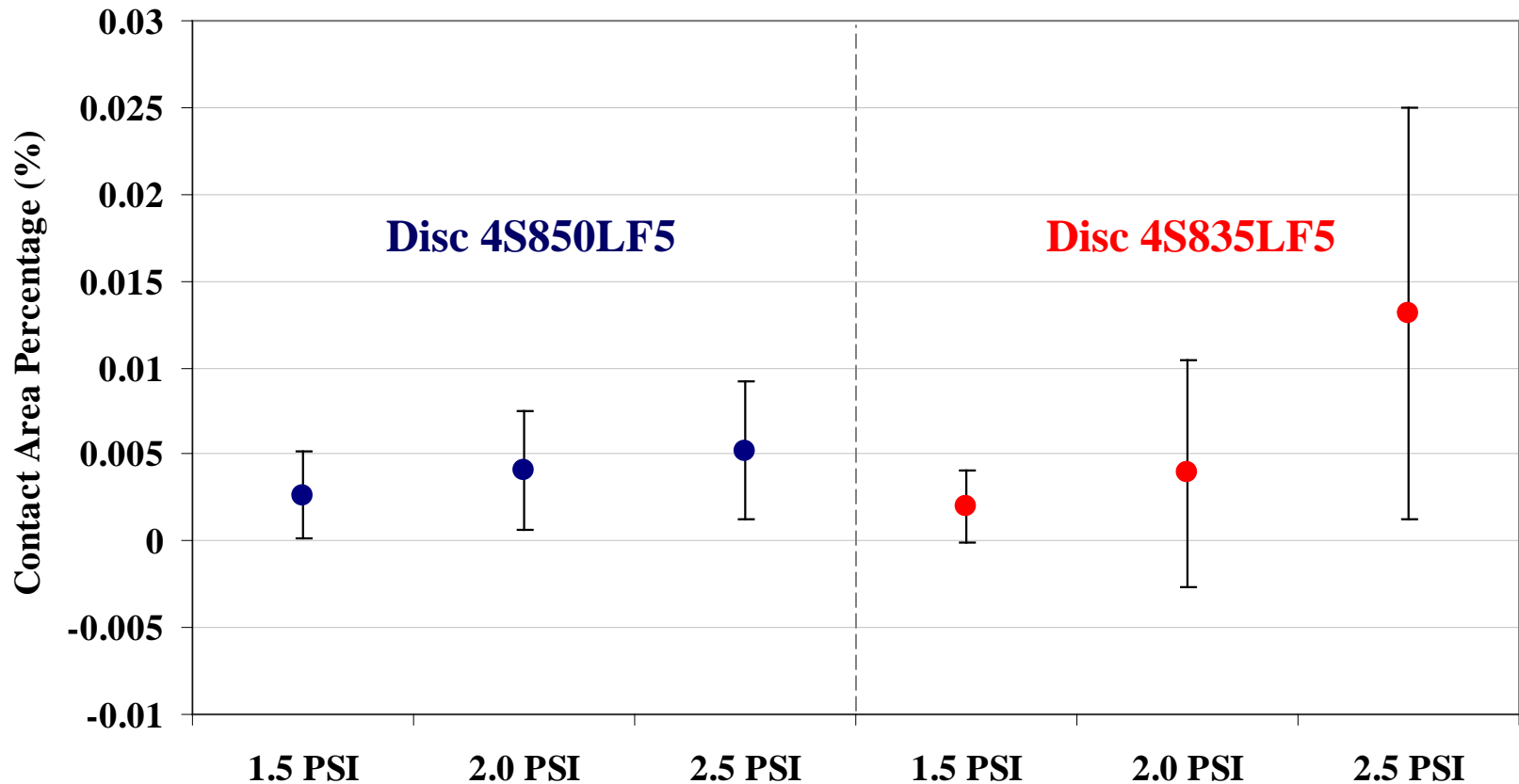
# Laser Confocal Microscope



Zeiss LSM 510 Meta NLO

**Pad surface contact area and topography were analyzed through laser confocal microscopy.**

# Pad Surface Contact Area Comparison

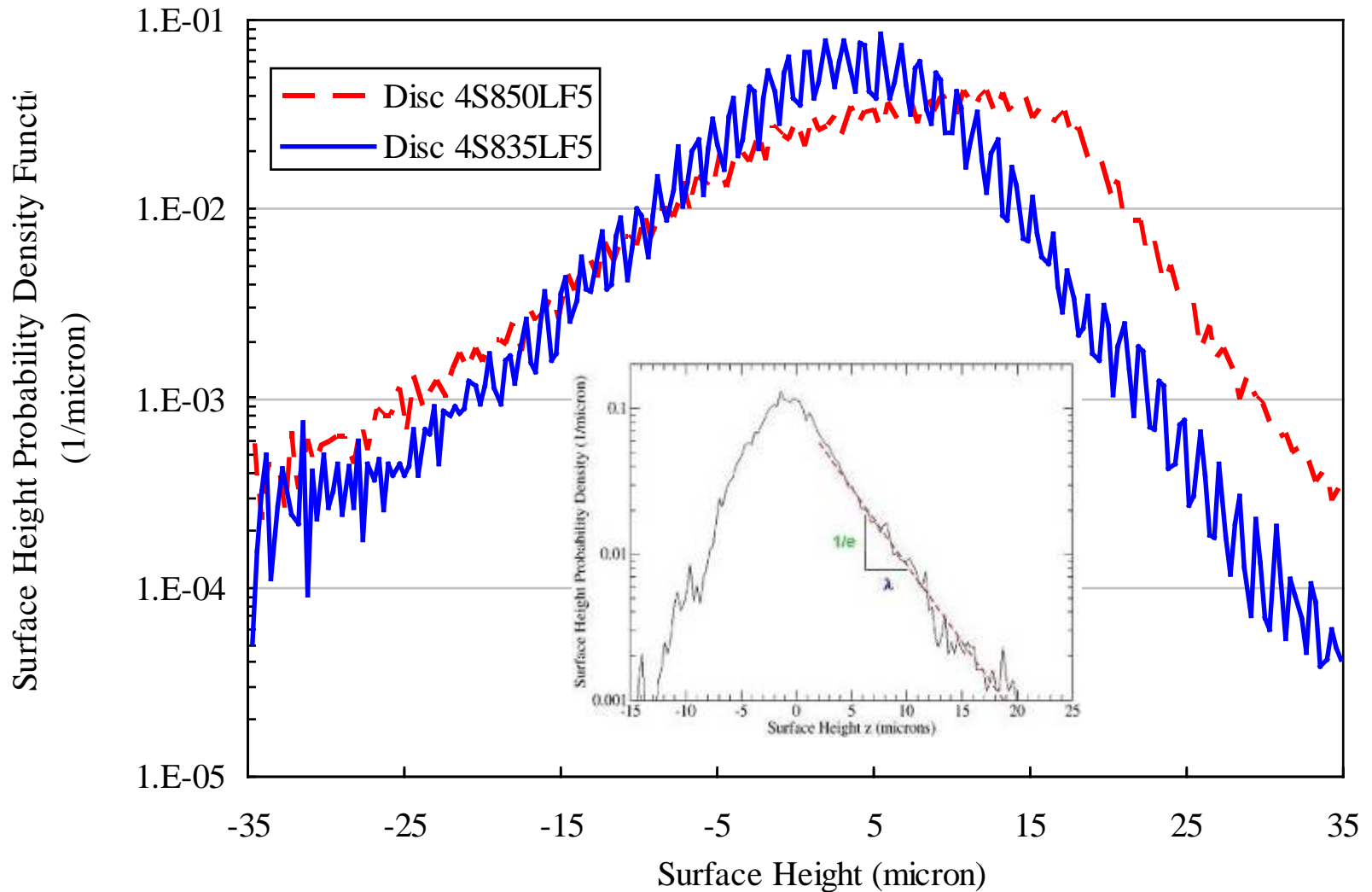


The two discs generated similar pad surface contact areas at 1.5 and 2.0 PSI.

Disc 4S850LF5 generated lower pad surface contact area than Disc 4S835LF5 at 2.5 PSI.

For both discs, pad surface contact area increased with pressure.

# Pad Surface Height Probability Density Functions



**Pad surface abruptness ( $\lambda$ ) was extracted from the pad surface height probability density function.**

## Pad Surface Abruptness Comparison

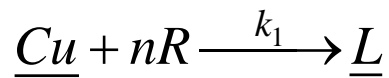
	$\lambda$ (micron)
Disc 4S850LF5	3.51
Disc 4S835LF5	4.25

**Disc 4S835LF5 generated a higher pad surface abruptness than Disc 4S850LF5. The larger pad surface abruptness resulted in higher coefficient of friction and removal rate for Disc 4S835LF5.**

# Two-Step Removal Rate Model

- **Modified Langmuir-Hinshelwood model:**

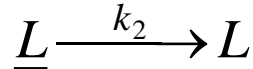
- **n moles of reactant R in the slurry react at rate  $k_1$  with copper film on the wafer to form a product layer  $\underline{L}$  on the surface**



$$k_1 = A \times \exp(-E_a / kT)$$

$$T = T_p + \frac{\beta}{V^{0.5+e}} \times COF \times p \times V$$

- **Product layer  $\underline{L}$  is subsequently removed by mechanical abrasion with rate  $k_2$**



$$k_2 = C_p \times COF \times p \times V$$

- **Abraded material  $\underline{L}$  is carried away by the slurry**

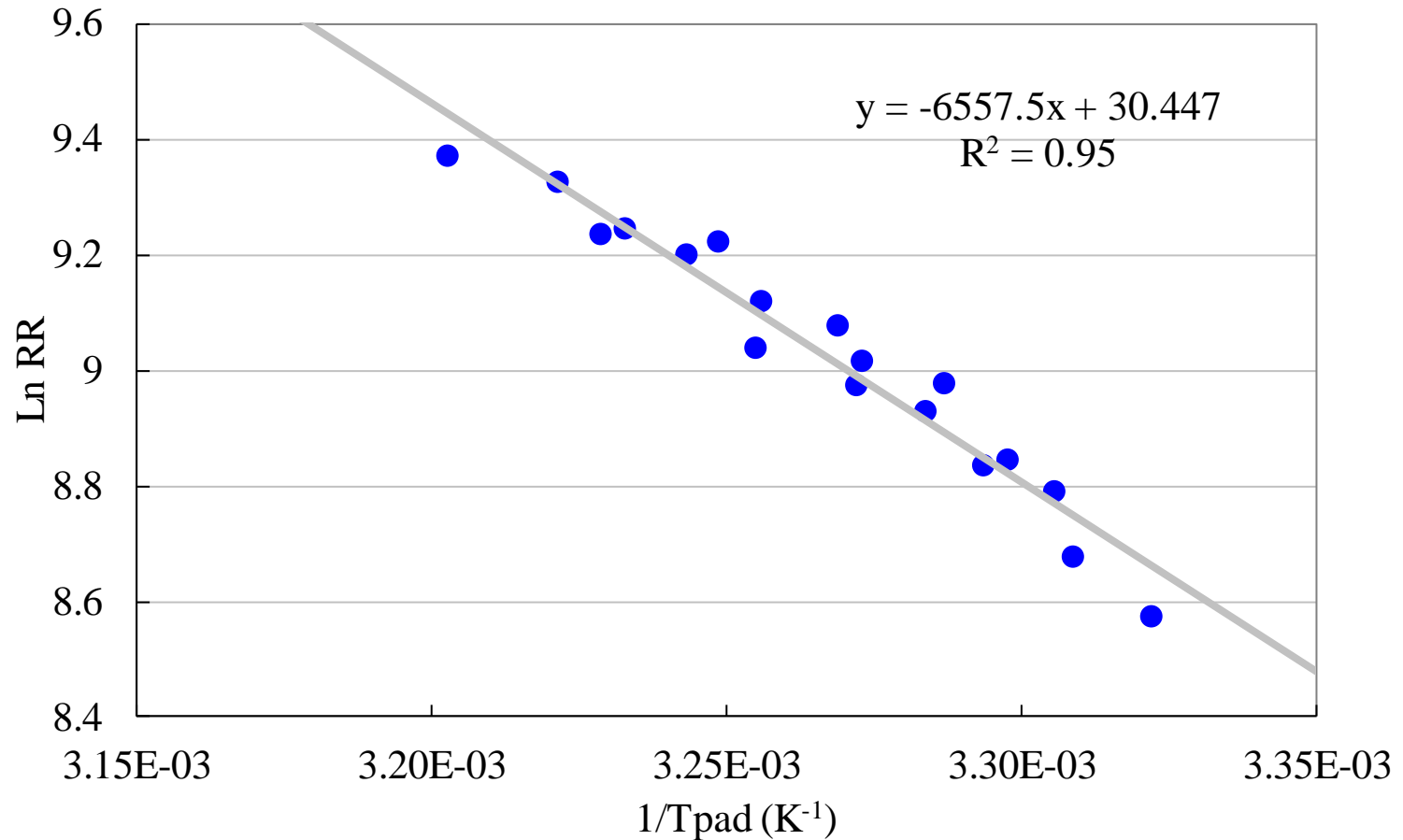
- **The removal rate in this sequential mechanism therefore is a function of both thermal and mechanical attributes of the process**

$$RR = \frac{M_w}{\rho} \frac{k_1 k_2}{k_1 + k_2}$$

# Fitting Parameters

$E_a$	<b>Slurry activation Energy (eV)</b>
$A$	<b>Pre-exponential factor of chemical rate constant (mole <math>\times</math> m<sup>-2</sup> s<sup>-1</sup>)</b>
$C_p$	<b>Proportionality constant of mechanical rate constant (mole/J)</b>
$e$	<b>Exponential factor of sliding velocity derived from pad heat partition fraction</b>
$\beta$	<b>A parameter that depends on wafer size, tool geometry and properties of pad surface and bulk material (10<sup>-3</sup> K/Pa(m/s)<sup>0.5-e</sup>)</b>

# Slurry Activation Energy Extraction



**The extracted slurry activation energy was 0.57 eV.**

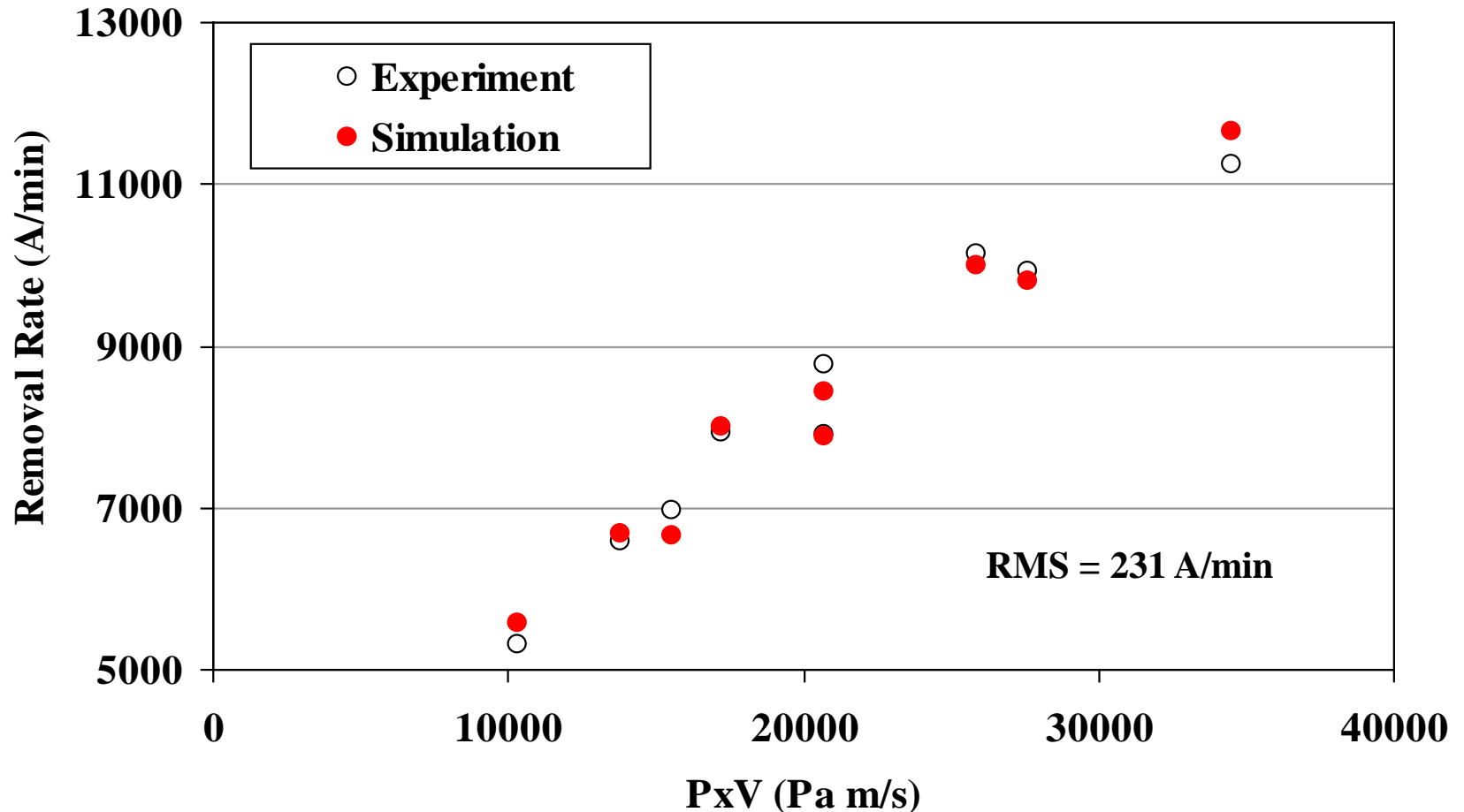
# Optimized Fitting Parameters

	<b>Disc 4S850LF5</b>	<b>Disc 4S835LF5</b>
<b><math>E</math> (eV)</b>	<b>5.70E-01</b>	<b>5.70E-01</b>
<b><math>A</math> (mole·m<sup>-2</sup>·s<sup>-1</sup>)</b>	<b>3.58E+06</b>	<b>3.58E+06</b>
<b><math>C_p</math> (mole/J)</b>	<b>2.15E-06</b>	<b>4.46E-06</b>
<b><math>e</math></b>	<b>8.20E-01</b>	<b>1.35E+00</b>
<b><math>\beta</math> (K/Pa(m/s)<sup>0.5-e</sup>)</b>	<b>3.09E-04</b>	<b>1.91E-04</b>

**Disc 4S835LF5 generated a higher proportionality constant of mechanical rate constant than Disc 4S850LF5.**

# Simulated Removal Rate

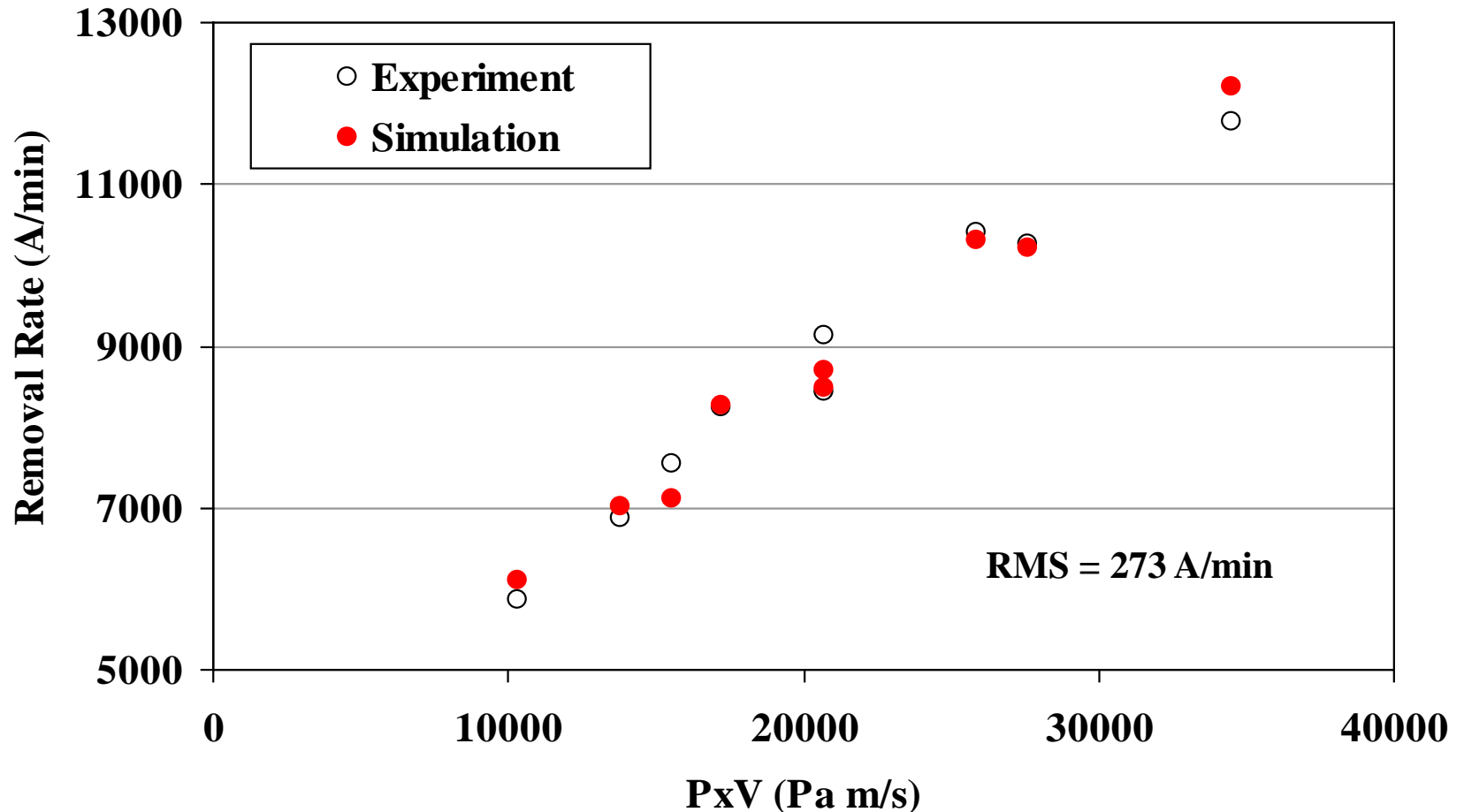
## Disc 4S850LF5



**Simulated removal rate agreed with the experimental data very well.**

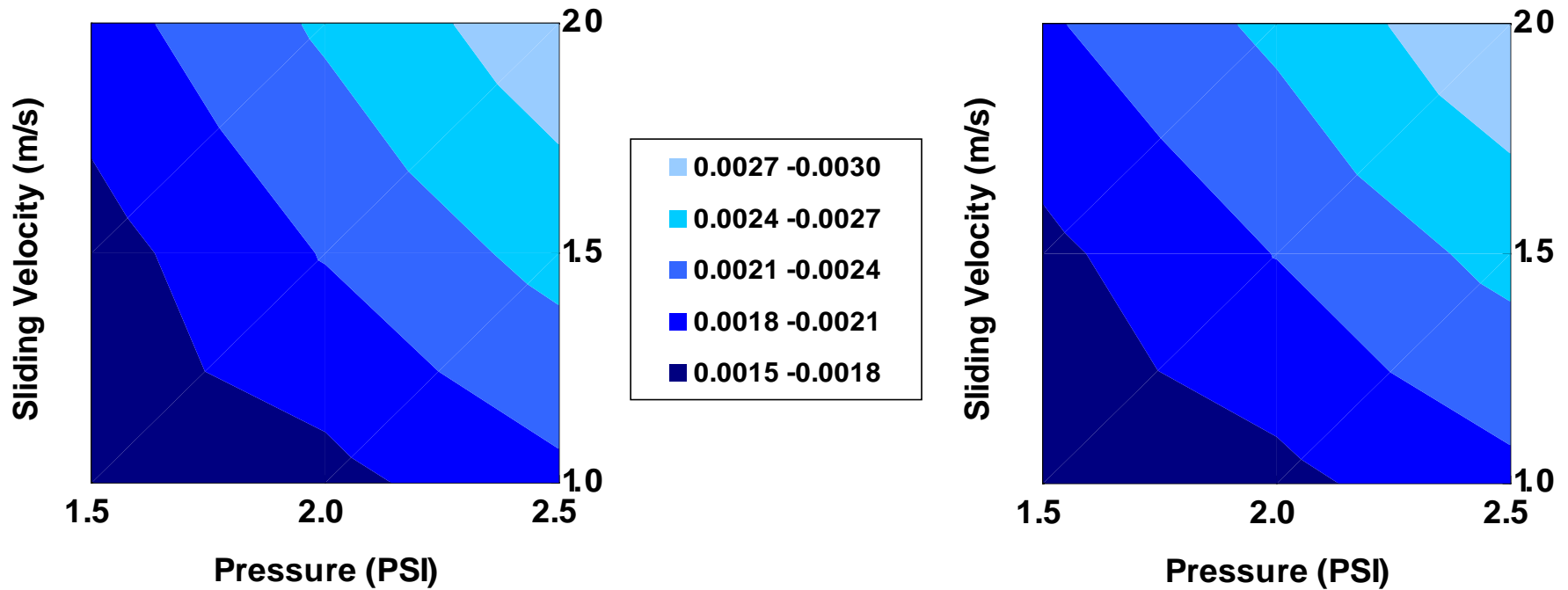
# Simulated Removal Rate

## Disc 4S835LF5



**Simulated removal rate agreed with the experimental data very well.**

# Lim-Ashby Plot of Chemical Rate Constants ( $k_1$ )

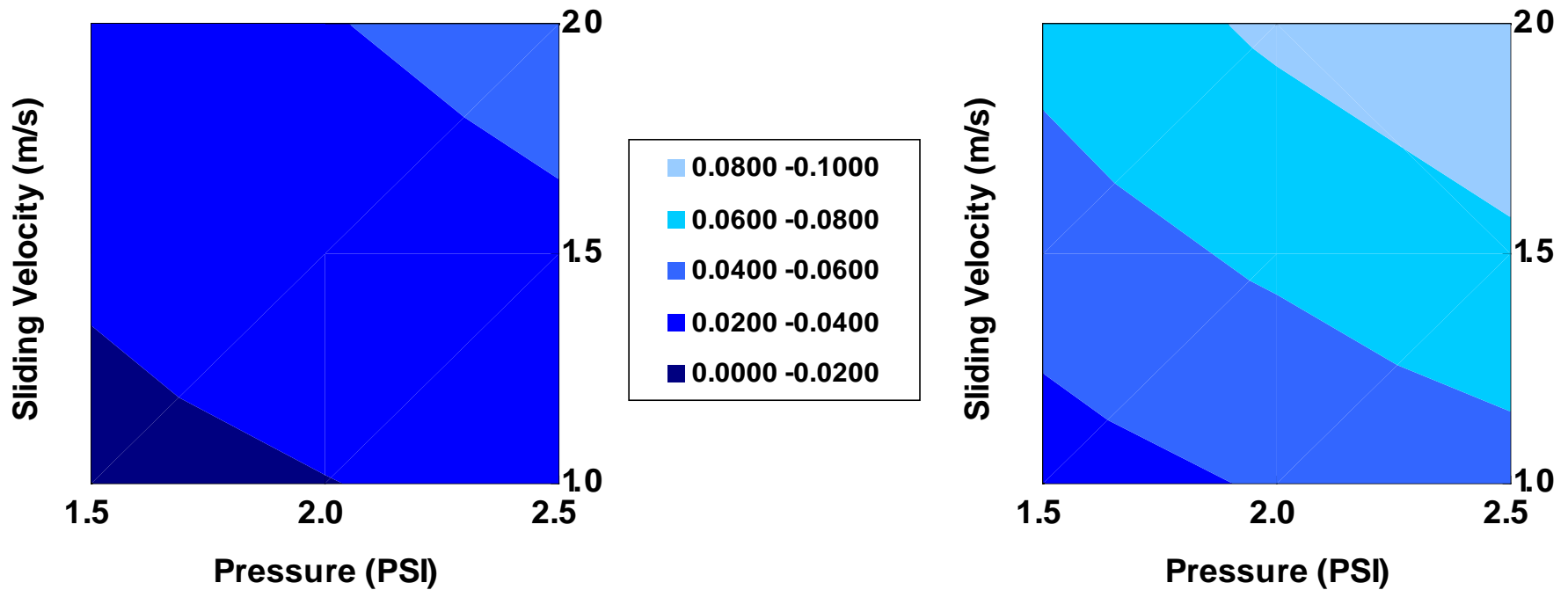


**Disc 4S850LF5**

**Disc 4S835LF5**

**4S850LF5 generated similar chemical rate constants ( $k_1$ ) compared to Disc 4S835LF5. For both discs, pressure and sliding velocity impacted on the chemical rate constant.**

# Lim-Ashby Plot of Mechanical Rate Constants ( $k_2$ )

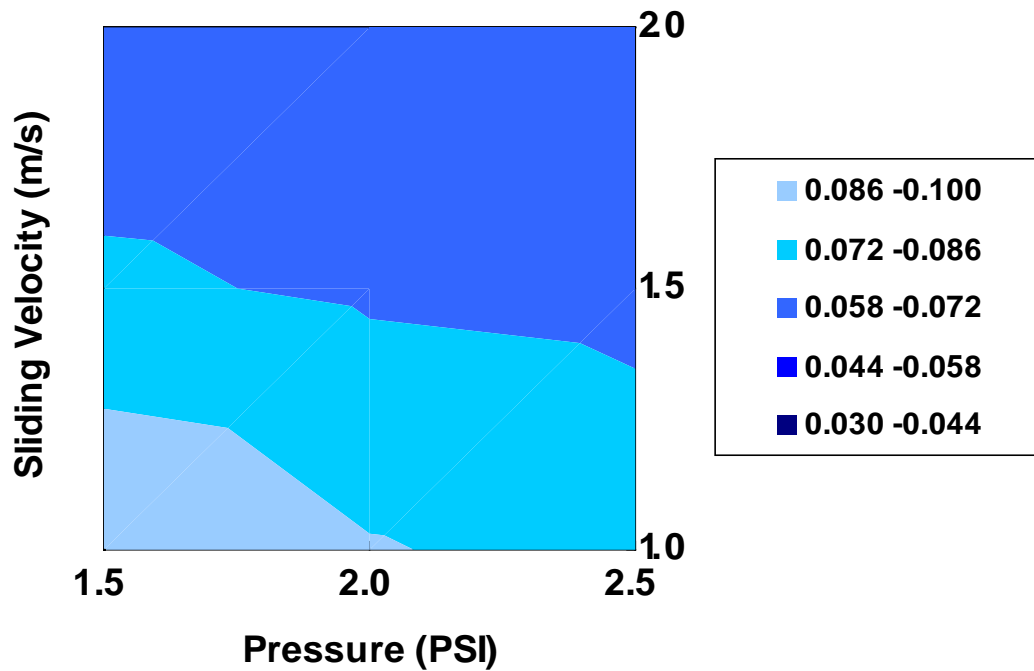


**Disc 4S850LF5**

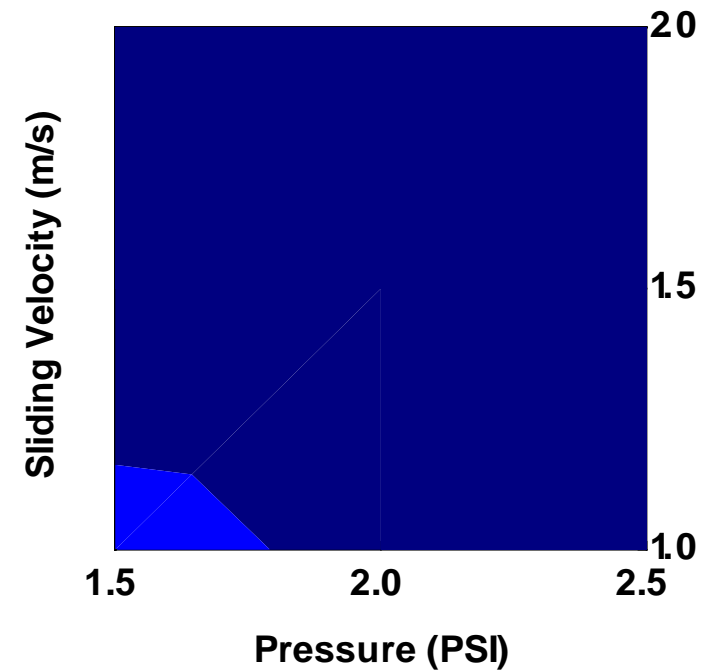
**Disc 4S835LF5**

Disc 4S835LF5 generated higher mechanical rate constants ( $k_2$ ) compared to Disc 4S850LF5. For both discs, pressure and sliding velocity impacted the mechanical rate constant. The higher mechanical rate constants contributed to higher copper removal rates for Disc 4S835LF5.

# Lim-Ashby Plot of Rate Constant Ratios ( $k_1/k_2$ )



**Disc 4S850LF5**



**Disc 4S835LF5**

Both discs generated  $k_1/k_2$  values that were significantly lower than 1, indicating that the polishing process was chemically limited. For both discs, at higher sliding velocities, pressure did not have significant impacts on the chemical to mechanical rate constant ratio.

## Summary

- **Disc 4S835LF5 generated a higher pad surface abruptness than 4S850LF5. The larger pad surface abruptness resulted in higher coefficient of friction and removal rate.**
- **The kinetic simulation indicated that Disc 4S850LF5 generated similar chemical rate constants compared to Disc 4S835LF5. On the other hand, Disc 4S835LF5 generated higher mechanical rate constants than Disc 4S850LF5. The higher mechanical rate constants contributed to higher copper removal rates for Disc 4S835LF5.**
- **The kinetic simulation showed that the polishing process was chemically limited for both discs. At higher sliding velocities, pressure did not have significant impacts on the chemical to mechanical rate constant ratio.**
- **We have achieved our goal of reducing CMP consumable consumption by 10% through removal rate increase with improved pad conditioning.**

# Industrial Interactions

## **Industrial mentors and contacts:**

- **Dave Slutz (Morgan Technical Ceramics)**
- **Cliff Spiro (Cabot Microelectronics Corporation)**
- **Ananth Naman (Cabot Microelectronics Corporation)**
- **Fred Sun (Cabot Microelectronics Corporation)**

## **Publications and Presentations**

- **Effects of Pad Micro-Texture on Frictional Force and Removal Rate during Copper CMP Process, X. Liao, Y. Zhuang, L. Borucki, S. Theng, T. Ashizawa and A. Philipossian. *Electrochemical and Solid-State Letters*, 14(5), H201-H204, 2011.**
- **An Approach for Correlating Friction Force and Removal Rate to Pad Topography during Tungsten Chemical Mechanical Planarization, Y. Sampurno, A. Rice, Y. Zhuang and A. Philipossian. *Electrochemical and Solid-State Letters*, 14(8), H318-H321, 2011.**
- **Correlation between Pad Surface Micro-Topography and Planarization in Copper CMP, Y. Jiao, Y. Zhuang, X. Liao, Y. Sampurno, C. Wu, S. Theng and A. Philipossian. *International Conference on Planarization/CMP Technology Proceedings*, 44-50, 2011.**
- **Correlation between Pad Surface Micro-Topography and Planarization in Copper CMP, Y. Jiao, Y. Zhuang, X. Liao, Y. Sampurno, C. Wu, S. Theng and A. Philipossian. *International Conference on Planarization/CMP Technology*, Seoul, Korea, November 9-11, 2011.**

## Publications and Presentations

- **Correlation of Pad Topography, Friction Force and Removal Rate during Tungsten Chemical Mechanical Planarization, Y. Sampurno, A. Rice, Y. Zhuang and A. Philipossian. ECS Transactions, 34(1), 621-626 2011.**
- **Correlation of Pad Topography, Friction Force and Removal Rate during Tungsten Chemical Mechanical Planarization, Y. Sampurno, A. Rice, Y. Zhuang and A. Philipossian. China Semiconductor Technology International Conference, Shanghai, China, March 13-14, 2011.**

# Fundamentals of Advanced Planarization: Pad Micro-Texture, Pad Conditioning, Slurry Flow, and Retaining Ring Geometry

*(Task 425.032)*

## Subtask 3: Implementation of an Extended Die-Level and Wafer-Level CMP Model

### PI:

- **Duane Boning, Electrical Engineering and Computer Science, MIT**

### Graduate Students:

- **Wei Fan, Ph.D. candidate, EECS, MIT**
- **Joy Johnson, Ph.D. candidate, EECS, MIT**

### Cost Share (other than core ERC funding):

- **Experimental support, Intel**

# Objectives

**Goal: Improve fundamental understanding of CMP thru modeling and experimentation of CMP consumables to:**

- **Reduce use of high-cost engineered consumables**
- **Reduce generation of by-product wastes**
- **Save processing times requiring significant energy**
- **Enable better process control**

## **1. CMP model integration**

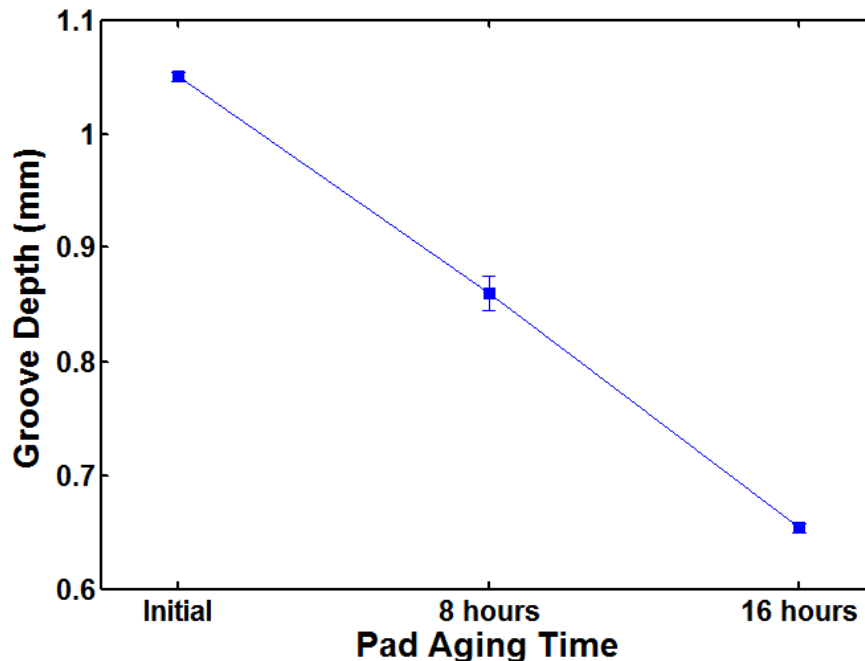
- **Extended wafer-level CMP model including polishing tool effects**
- **Extended die-level CMP model including pad surface properties**

## **2. Slurry agglomeration modeling**

# Extended Wafer-Level CMP Model

- **Extended wafer-level CMP model including polishing tool effects**
  - **Retaining ring effects on wafer edge pressure distributions**
  - **Pad thickness changes: examine pattern wafer effects due to finite (and changing) pad thickness**

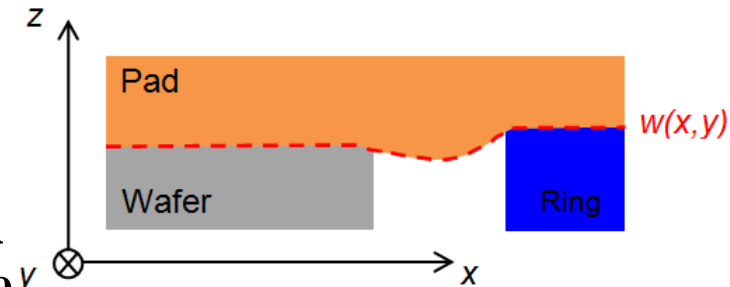
**Pad wear  
during CMP  
process**



*Fan, et al., ICPT 2011*

# Modeling of Wafer-Level Pressure Distribution

- The pad is assumed to be an elastic body with finite thickness
- Wafer and retaining are both rigid
- The relationship between pad deformation and wafer/retaining ring surface topography can be calculated using a contact wear model



**Pad Surface Displacement**

$$\bar{w}(\xi_m, \eta_n) = \bar{C}(\xi_m, \eta_n) \cdot \bar{P}(\xi_m, \eta_n)$$

Discrete Fourier transform

$$\bar{w}(\xi_m, \eta_n) = \sum_{m=0}^N \sum_{n=0}^N e^{-i(\xi_m x + \eta_n y)} w(x, y) \quad \bar{P}(\xi_m, \eta_n) = \sum_{m=0}^N \sum_{n=0}^N e^{-i(\xi_m x + \eta_n y)} P(x, y)$$

**Influence coefficient**

$$\bar{C}(\xi_m, \eta_n) = -\left(\frac{1-\nu}{u}\right) \left(1 + 4\alpha h k e^{-2\alpha h} - \lambda k e^{-4\alpha h}\right) \alpha R \quad h: \text{pad thickness}$$

**Boundary Conditions**

$$\begin{cases} P(x, y) \geq 0 \\ \frac{1}{S_0} \int_{\text{wafer}} P(x, y) \cdot dx \cdot dy = P_0 \\ \frac{1}{S_r} \int_{\text{ring}} P(x, y) \cdot dx \cdot dy = P_r \\ w(x, y) \geq z(x, y) \end{cases}$$

Pressure can not be negative

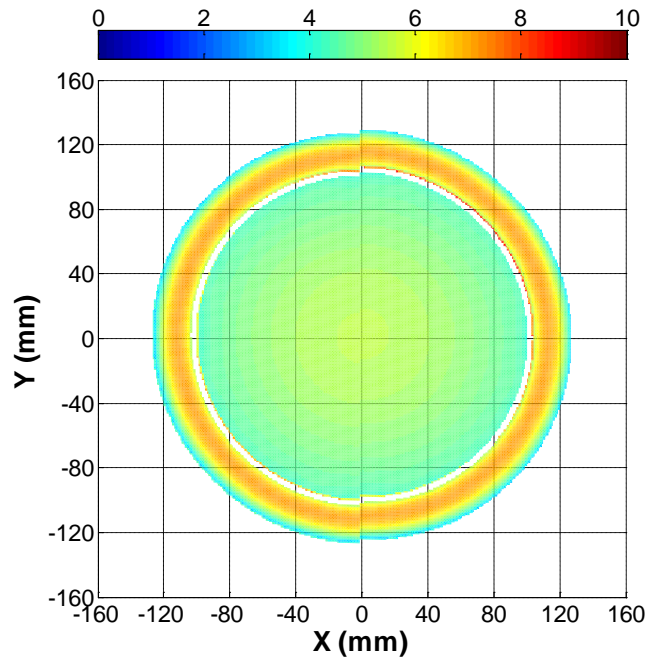
Average wafer pressure equals to wafer reference pressure

Average ring pressure equals to ring reference pressure

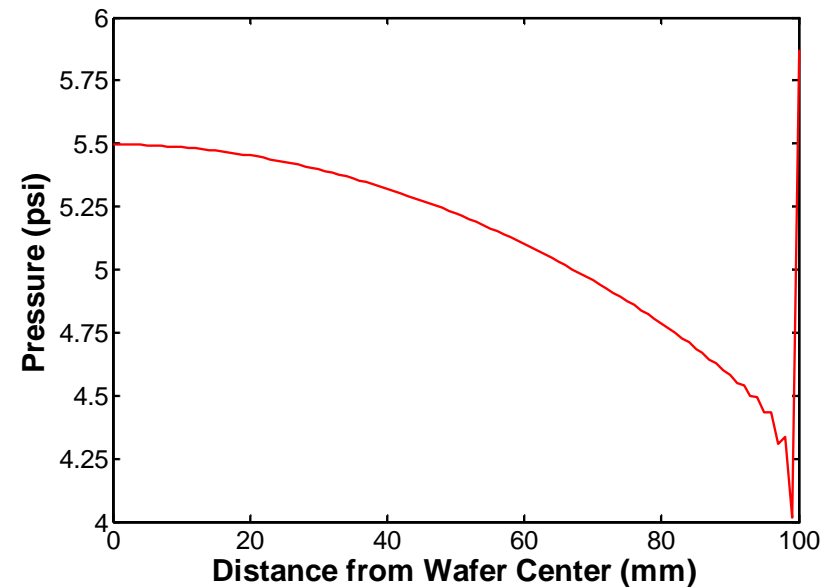
$z(x, y)$ : surface of wafer and ring structure

# Wafer-Level Pressure Non-uniformity

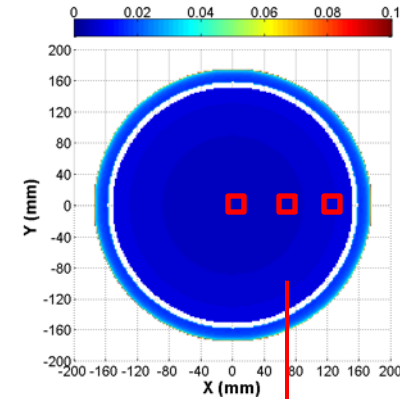
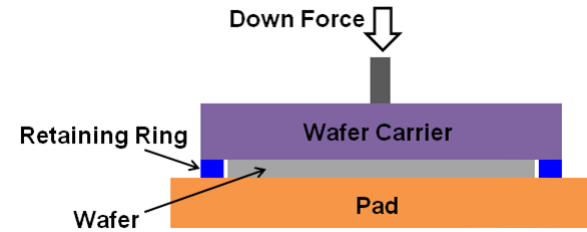
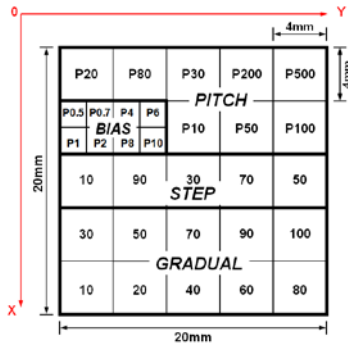
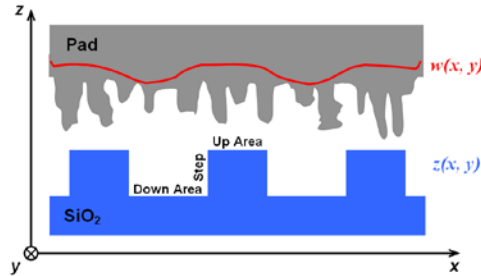
**Pressure distribution on wafer and retaining ring**



**Pressure distribution along wafer radius**



# Wafer-Level Model Integration



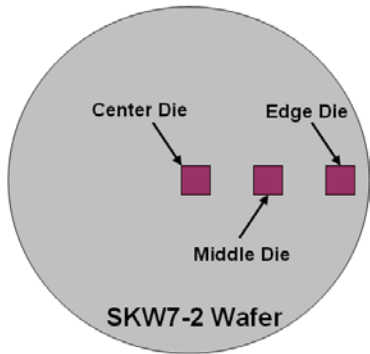
Local pressure boundary condition

$$\begin{cases}
 w(x, y) = F(x, y) \otimes P(x, y) + w_0 \\
 P_d(x, y) = \frac{1}{1 + \rho(x, y) \cdot \left( e^{\frac{h(x, y)}{\lambda}} - 1 \right)} P(x, y) \\
 P_u(x, y) = \frac{e^{\frac{h(x, y)}{\lambda}}}{1 + \rho(x, y) \cdot \left( e^{\frac{h(x, y)}{\lambda}} - 1 \right)} P(x, y)
 \end{cases}
 \left\{ \begin{array}{l}
 P(x, y) \geq 0 \\
 \frac{1}{S} \int_S P(x, y) \cdot dx \cdot dy = P_{local} \\
 w(x, y) \geq z(x, y)
 \end{array} \right.$$

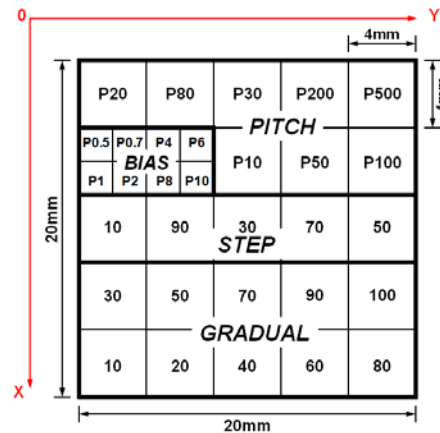
# Model Fitting

## • Patterned oxide wafer polishing with JSR pad

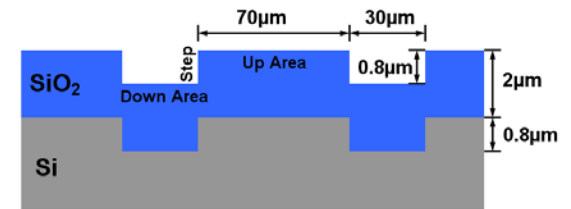
Measured die positions on a SKW7-2 dielectric wafer



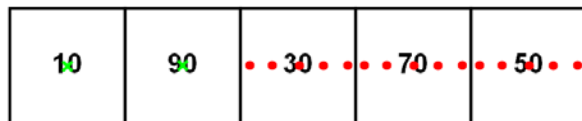
Layout of a die on SKW7-2 wafer



Topography of the 70% STEP array



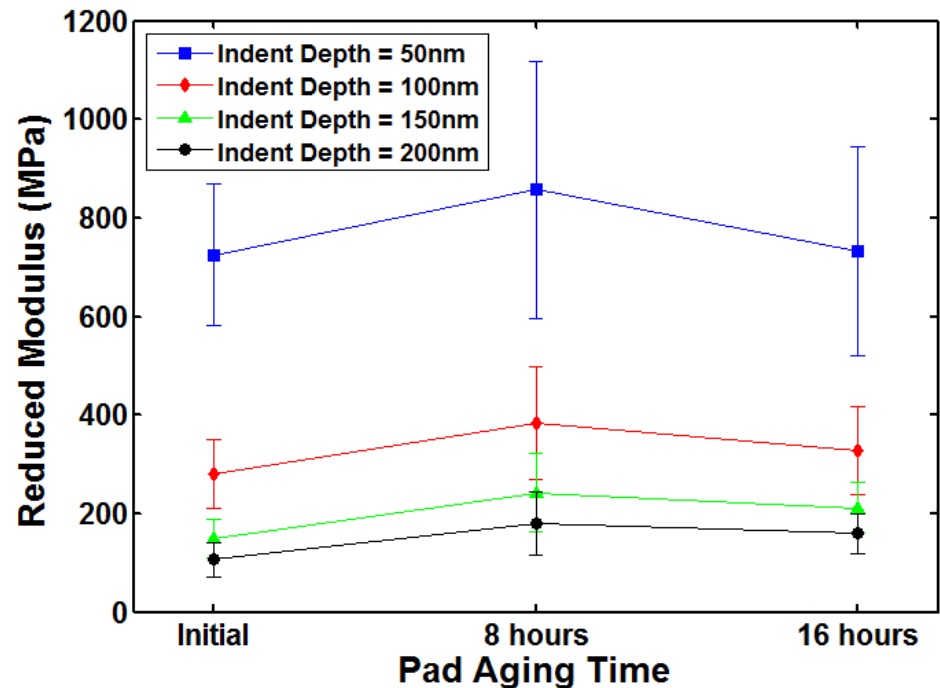
Measurement positions in the STEP blocks in a die of SKW7-2 dielectric wafer



- Step height and film thickness measured at:  
t=0s, t=20s, t=40s, t=70s, t=90s, t=110s, t=130s
- ✗ Step height measured at:  
t=0s, t=20s, t=40s, t=70s, t=90s, t=110s, t=130s

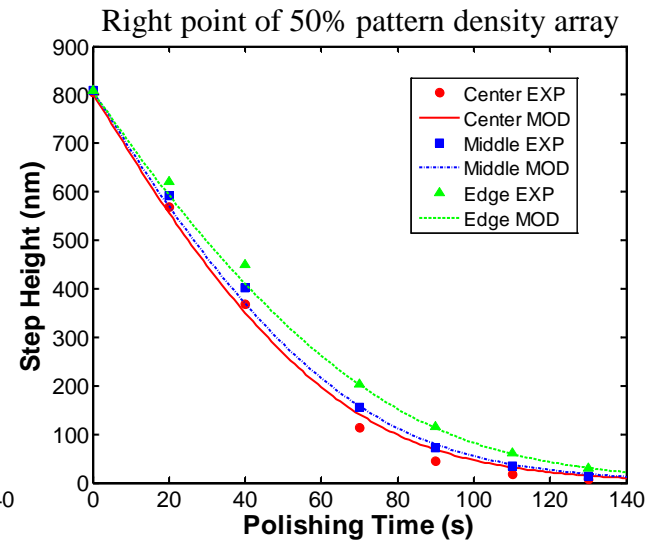
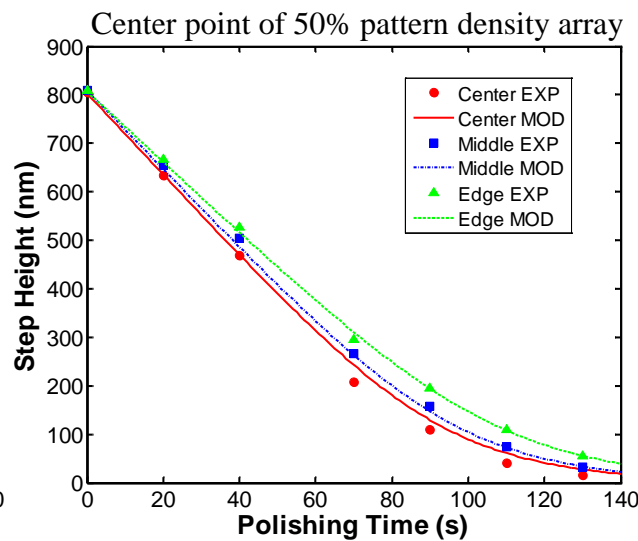
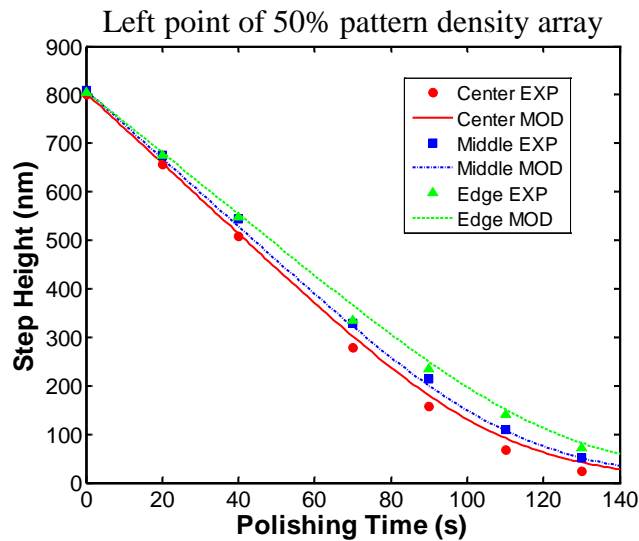
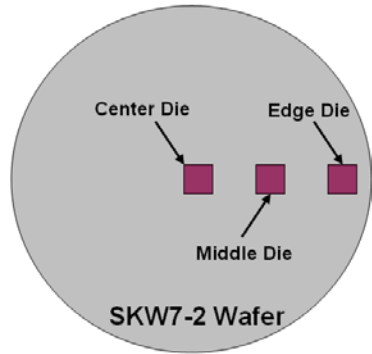
# Extracted Model Parameters

- Blanket removal rate:  $K_0 = 224.3$  nm/s
  - Characteristic asperity height:  $\lambda = 97.4$  nm
  - Pad bulk effective modulus:  $E_b = 141.5$  MPa
  - Pad surface effective modulus:  $E_s = 271.2$  MPa
- 
- Contact induced stiffening
    - Find that  $E_s > E_b$



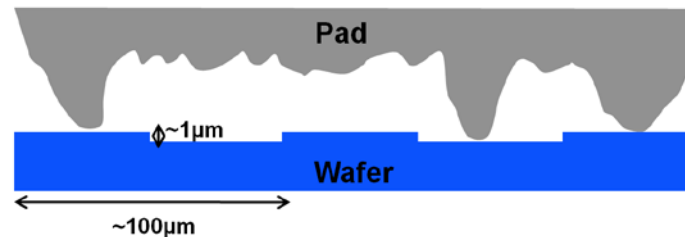
Fan, et al., ICPT 2011

# Wafer-Level Non-uniformity Impact on Die-Level Step-height Evolution

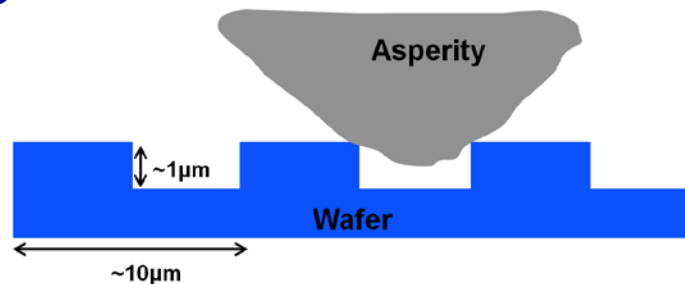


# Extended Die-Level CMP Model

- **Objective**
  - Consider asperity contact with patterned wafer
  - Include feature size effect
- **Same pattern density**
  - Large feature size



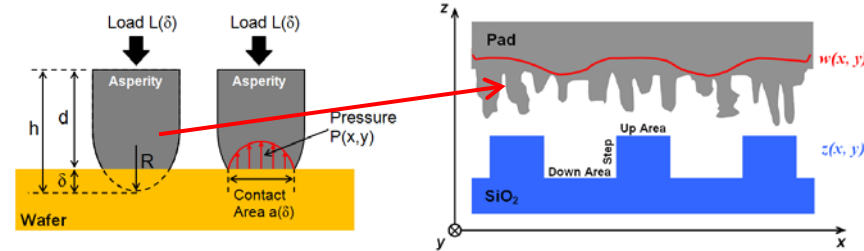
- Small feature size



# Model Approach

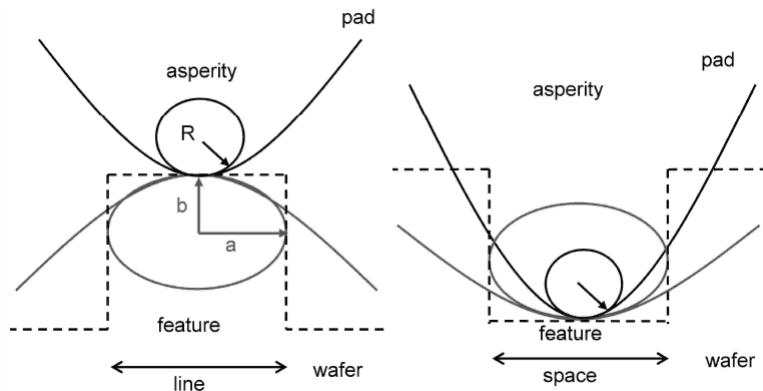
- **Greenwood Williamson approach**

- Asperities have spherical surfaces with same radius
- Elastic Hertzian contact



- **Geometry of Hertzian contact**

- Both asperity and wafer surfaces are described by parabolic shapes



Vasilev, IEEE Trans. on Semiconductor Manufacturing 2011

$$\kappa^{U,D} = \frac{1}{R_{\text{asperity}}} \pm \frac{1}{R_{\text{feature}}} = \kappa_{\text{asperity}} \pm \kappa_{\text{feature}}$$

$$\kappa_{\text{feature}} = \kappa_{\text{ellipse}} = \frac{b}{a^2}$$

$$\kappa^U = \kappa_{\text{asperity}} + \frac{4\alpha h}{\text{line}^2}$$

$$\kappa^D = \kappa_{\text{asperity}} - \frac{4\alpha h}{\text{space}^2}$$

# Model Trend

## Extended die-level model

$$\left\{ \begin{array}{l} w(x, y) = F(x, y) \otimes P(x, y) + w_0 \\ P_U(x, y) = \frac{e^{\frac{h}{\lambda} \kappa_U \sqrt{\kappa_D}}}{\kappa_{asp} \left( \sqrt{\kappa_U} (1 - \rho) + e^{\frac{h}{\lambda} \sqrt{\kappa_D} \rho} \right)} P(x, y) \\ P_D(x, y) = \frac{\kappa_D \sqrt{\kappa_U}}{\kappa_{asp} \left( \sqrt{\kappa_U} (1 - \rho) + e^{\frac{h}{\lambda} \sqrt{\kappa_D} \rho} \right)} P(x, y) \end{array} \right.$$

$$\begin{aligned} \kappa^U &= \kappa_{asperity} + \frac{4\alpha h}{line^2} \\ \kappa^D &= \kappa_{asperity} - \frac{4\alpha h}{space^2} \end{aligned}$$

Asperity size decreases



Pitch size increases

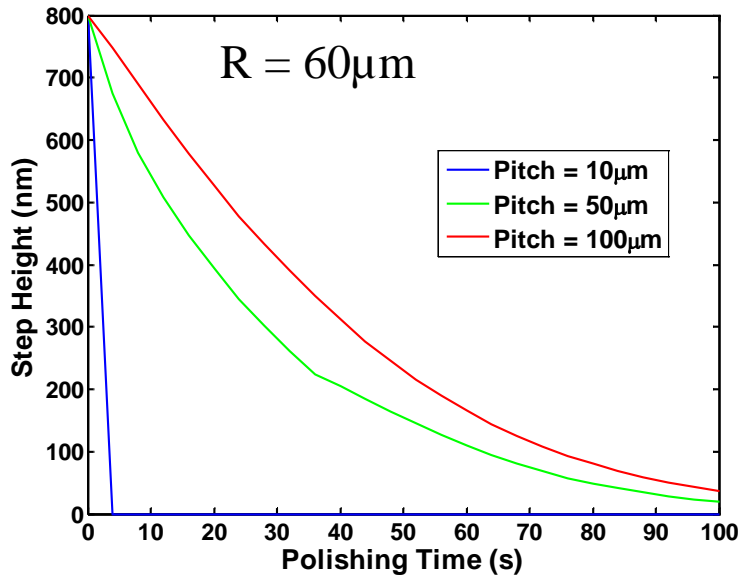
## Original die-level model

$$\left\{ \begin{array}{l} w(x, y) = F(x, y) \otimes P(x, y) + w_0 \\ P_u(x, y) = \frac{e^{\frac{h(x,y)}{\lambda}}}{1 + \rho(x, y) \cdot \left( e^{\frac{h(x,y)}{\lambda}} - 1 \right)} P(x, y) \\ P_d(x, y) = \frac{1}{1 + \rho(x, y) \cdot \left( e^{\frac{h(x,y)}{\lambda}} - 1 \right)} P(x, y) \end{array} \right.$$

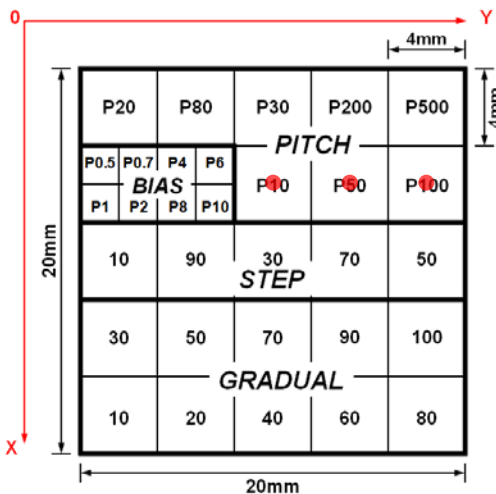
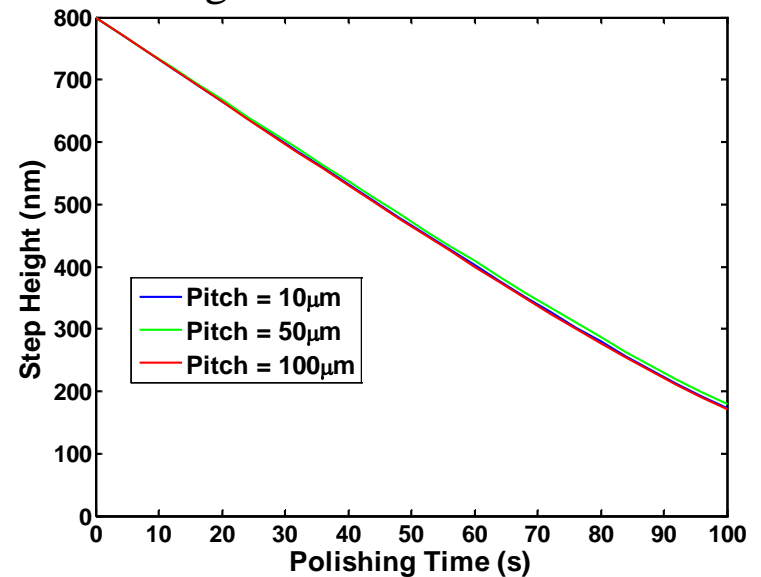
*Fan and Boning, Journal of The Electrochemical Society, 157, 2010*

# Feature Size Effect Simulation – Step Height

Extended Die-Level Model



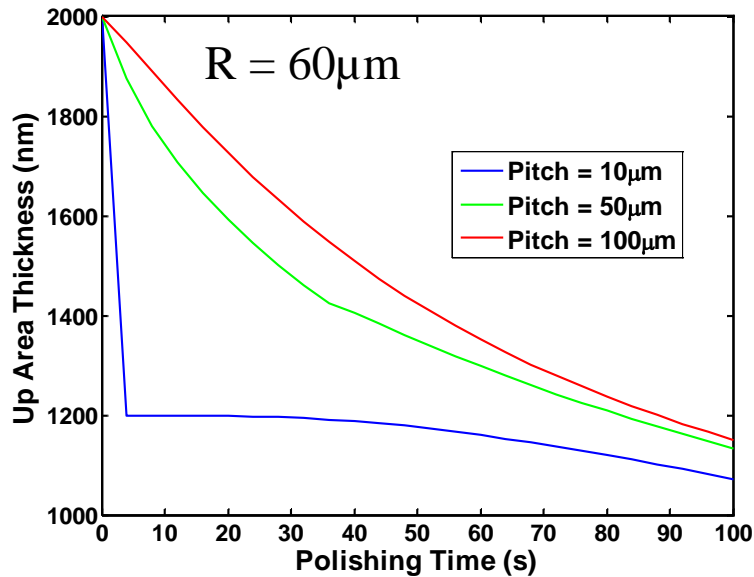
Original Die-Level Model



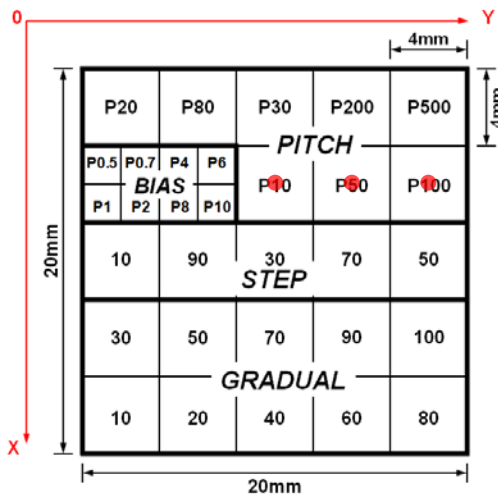
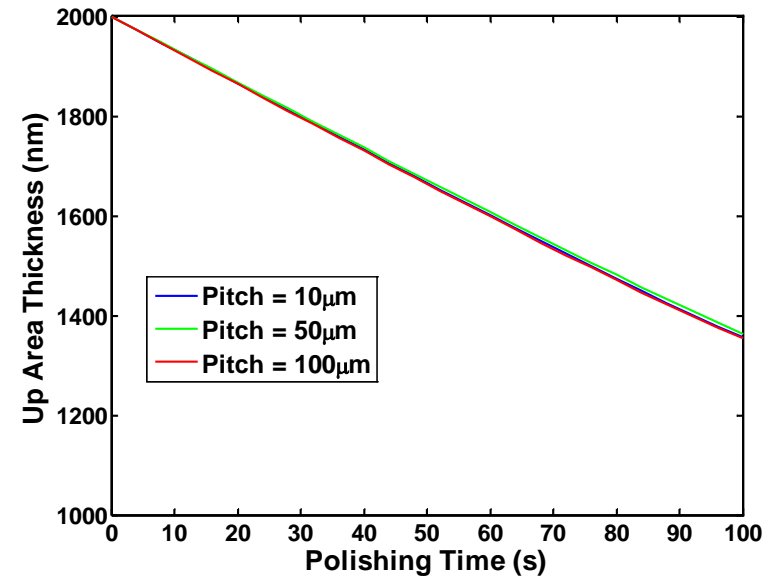
- Extended model has feature size dependence
  - Within same density region, step height of small size features reduces fast
- Original model has no feature size dependence

# Feature Size Effect Simulation – Up Area Polish

Extended Die-Level Model



Original Die-Level Model

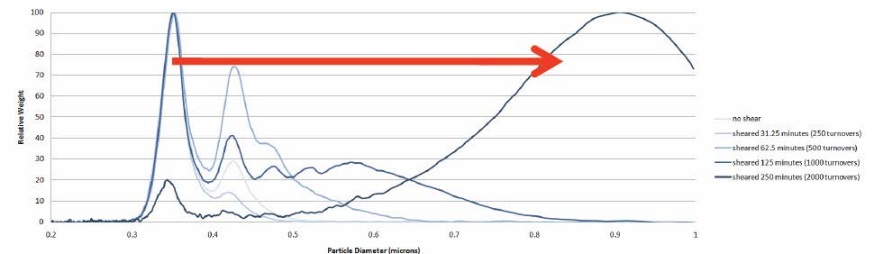
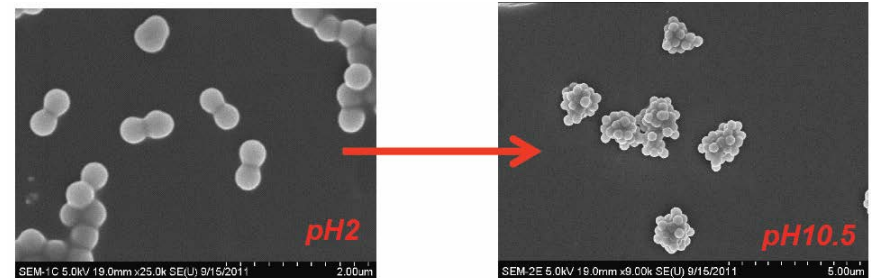


- Extended model has feature size dependence
  - Within same density region, up area thickness of small size features reduces very quickly
- Original model has no feature size dependence

# Slurry Agglomeration Modeling

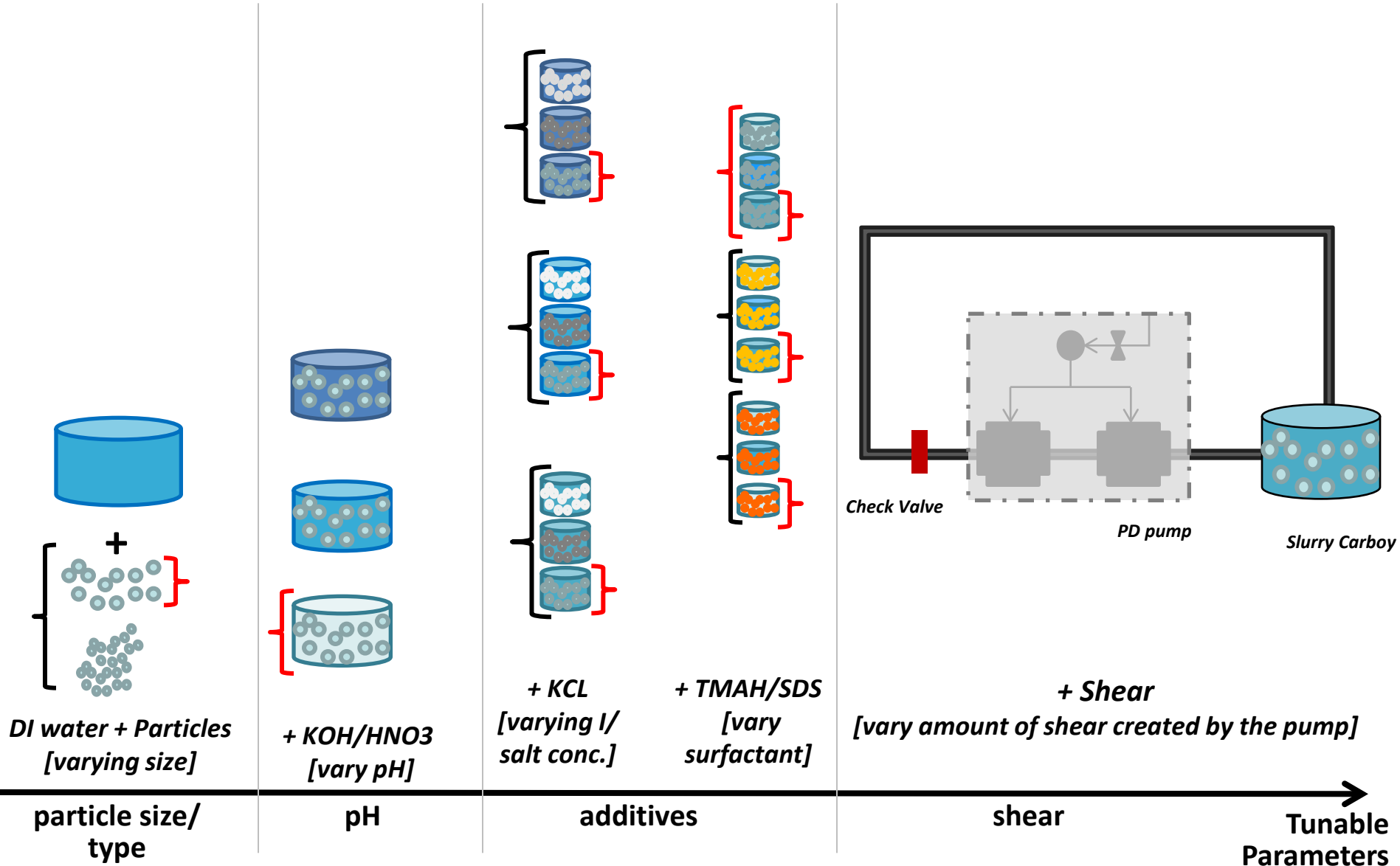
**Issue: Slurry chemistry, process conditions, and tool design affect slurry particle size and agglomeration – poor slurry utilization to avoid defectivity**

- **Agglomeration model development:**
  - Account for slurry particles, and wafer debris in the creation of agglomerates (respective of size and composition)
  - Account for slurry stability based on agglomerates, chemical composition, and shear forces during CMP
  - Calculate probability of agglomerate size distribution and corresponding stability
- **CMP model/experimental investigations:**
  - Slurry particle size distribution and stability
  - Slurry chemistry dependence (pH and zeta potential)
  - Shear conditions



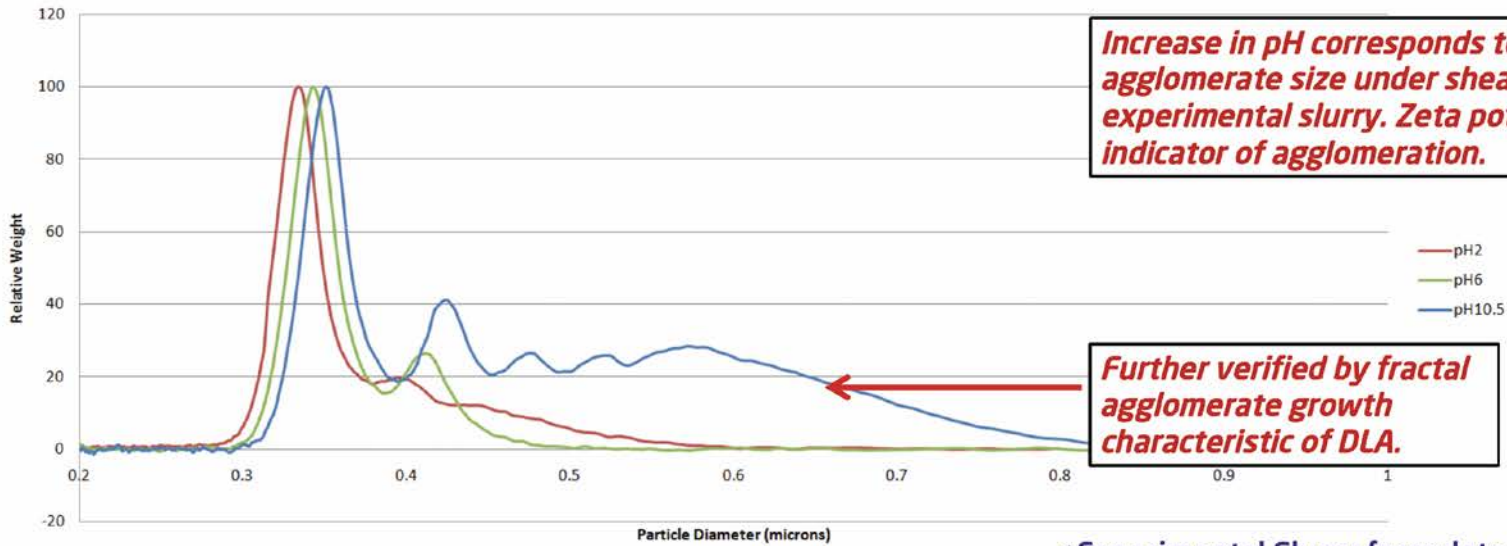
**CMP Time: 0-20 seconds**

# Design of Experiments



# Experimental Results

Disc Centrifuge Results: .15wt% PL-20[5 wt%] + 1M KCl + shear (125 min./1000 turnovers)

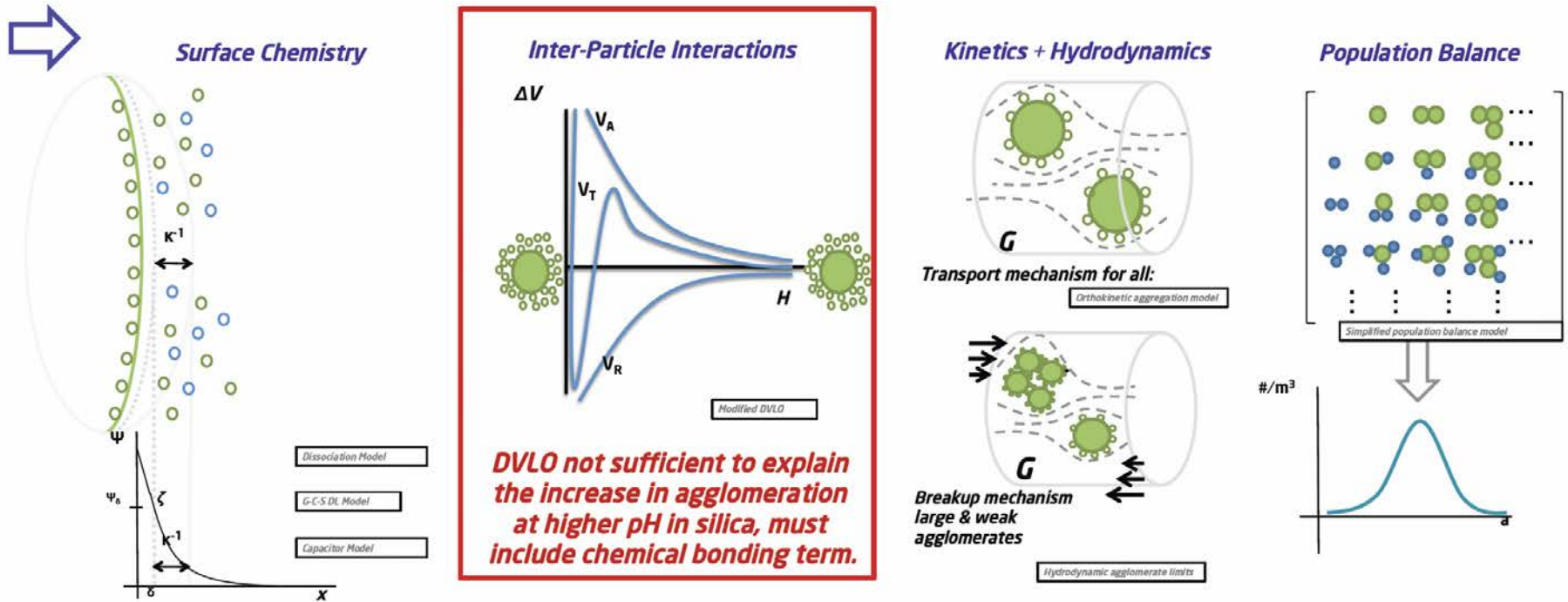


*Increase in pH corresponds to increase in agglomerate size under shear even in simple experimental slurry. Zeta potential NOT an indicator of agglomeration.*

*Further verified by fractal agglomerate growth characteristic of DLA.*

\*Experimental Slurry formulated by J.Johnson at Intel

# Slurry Agglomeration Model Implications

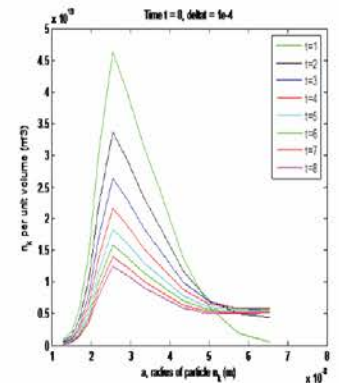
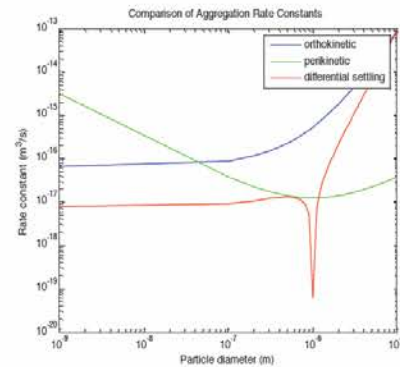
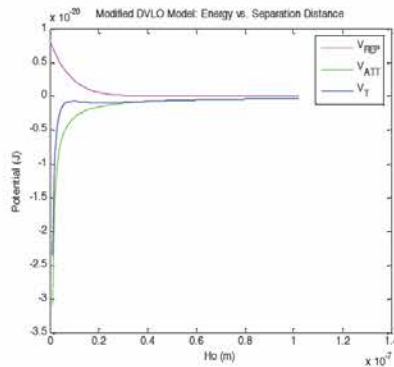
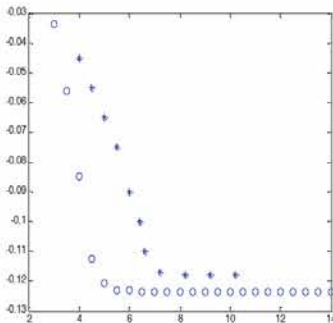


Zeta Potential,  $\zeta$   
Surface charge density,  $\sigma$

Collision efficiency,  $W$

Collision efficiency,  $J(\Delta n)$

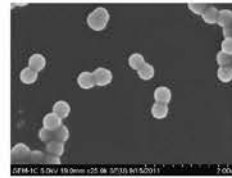
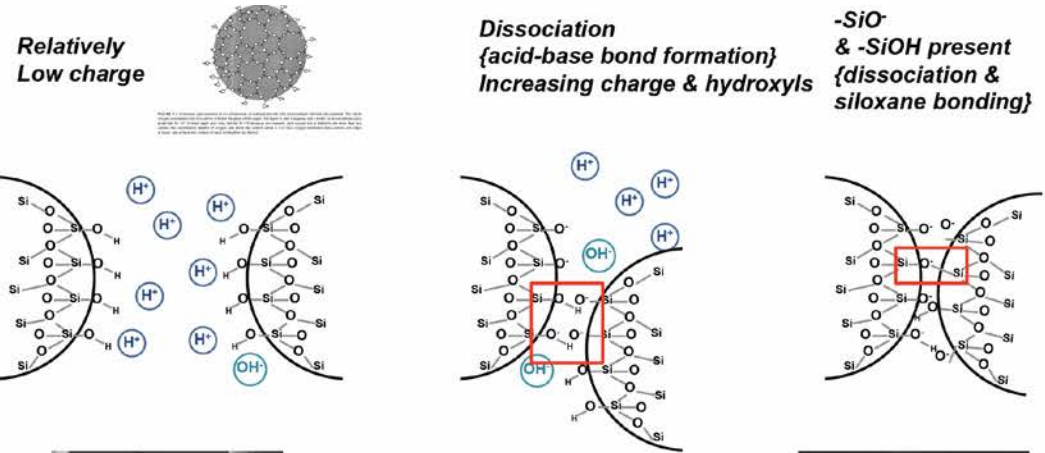
Particle Size Distribution



# Improved Model – Agglomeration Mechanism

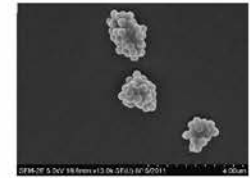
- Illustration at right shows the accepted behavior of silica as pH is increased. Agglomeration increases from the formation of interparticle acid-base bonds, which can transform in alkaline media to more stable siloxane bonds.

- Below is a comparison of the mean particle size of pH 2 and pH 10.5 samples under shear, and our model.



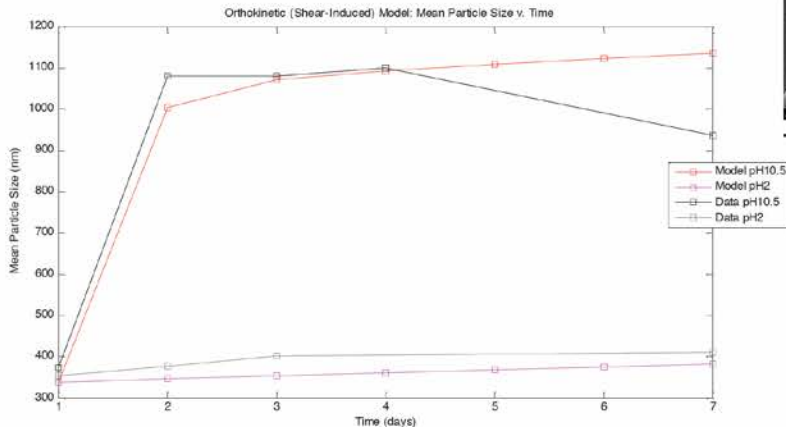
2

6



10.5\*

pH  
Decrease in [H<sup>+</sup> ions]  
Increase in hydroxyl groups  
OH<sup>-</sup> increase



# Summary

- **Developed extended wafer-level CMP model including retaining ring and polishing tool effects: guidance**
- **Developed extended die-level CMP model coupling pad properties to polishing performance**
- **Integrated wafer-level and die-level CMP models, to predict and jointly optimize wafer-level uniformity with die-level product wafer impact**
- **Developed slurry agglomeration modeling approach, with application to slurry design, polish condition optimization, and future applications such as pad in a bottle development**
- **Identified driver for agglomeration bond formation, for improved agglomeration model**

# Industrial Interactions

- **Cabot Microelectronics – Wei Fan, summer 2011 internship**
- **Intel – Joy Johnson, summer/fall 2011 internship**

# Publications and Presentations

- **W. Fan, D. Boning, Y. Zhuang, Y. Sampurno, A. Philipossian, M. Moinpour, and D. Hooper, “Characterization of CMP Pad Surface Properties and Aging Effects,” International Conference on Planarization Technology (ICPT), Seoul, Korea, Nov. 2011.**
- **J. Johnson, D. Boning, G.-S. Kim, R. Mudhivarathi, P. Safier, K. Knutson, and K. Pate, “Slurry Particle Agglomeration Model for Chemical Mechanical Planarization (CMP),” International Conference on Planarization Technology (ICPT), Seoul, Korea, Nov. 2011.**